Cover Page

Universiteit Leiden

Leiden University Repository

The handle http://hdl.handle.net/1887/138670 holds various files of this Leiden University dissertation.

Author: Gagestein, B.
Title: Chemical tools to study lipid signaling
Issue Date: 2020-12-16

Chapter 3

Bioorthogonal photoaffinity probes of omega-3 signaling lipids reveal PTGR1 as a metabolic hub in human macrophages*

Introduction

Dietary omega-3 polyunsaturated fatty acids (PUFAs) are generally considered to be beneficial for human health.[1–3] For example, the fish oil constituent docosahexaenoic acid (DHA, 22:6 n-3, **1**) is important for brain development, neuronal protection and the immune system (Scheme 1A).[2–7] Mechanistic studies indicate that many of the favorable effects of omega-3 fatty acids are due to their interaction with immunological processes,[1,2] which has been reiterated by the discovery of their oxidized metabolites involved in the resolution of inflammation.[8,9] Malfunction of this resolution phase of inflammation is hypothesized to contribute to many chronic inflammatory diseases, such as rheumatoid arthritis and asthma.[10,11] A better molecular understanding of the biological role of these lipids in the resolution phase of inflammation is required to develop therapeutics for these diseases.

*The data presented in this chapter was gathered in collaboration with Joost von Hegedus, Joanneke C. Kwekkeboom, Marieke Heijink, Bogdan I. Florea, Hans van den Elst, Kim Wals, Herman S. Overkleeft, Martin Giera, René E. M. Toes, Andreea Ioan-Facsinay, Mario van der Stelt.

The resolution of inflammation requires the intricate orchestration of cells of the innate immune system via soluble mediators. Among these, oxidative metabolites of DHA play a central role.[7,12] Biochemical studies have shown that DHA is oxidized into a central precursor, 17-hydroxy-docosahexaenoic acid (17-HDHA, **2**) via multiple pathways, including 15-lipoxygenase and cyclooxygenase acetylated by aspirin (Scheme 1A).[13] Oxidation by 15-lipoxygenase results in the formation of 17(S)-HDHA, while acetylated COX generates 17(R)-HDHA.[14] Importantly, 17-HDHA has protective effects in various animal models of colitis, arthritis and renal reperfusion.[15–18] *In vitro,* human macrophages produce less TNFα and more IL-10 following exposure to 17-HDHA.[19,20] Treatment with 17-HDHA also reduces LTB4 production in both isolated murine and human neutrophils.[20,21] Moreover, 17-HDHA can be further metabolized to specialized proresolving lipid mediators (SPMs), such as D-series resolvins and protectins (Scheme 1A), a process involving several enzymes. Resolvins and protectins are bioactive lipids with potent pro-resolving activities, including halting the infiltration of neutrophils and enhancing the non-phlogistic clearance of apoptotic cells, cellular debris and microbes by macrophages, thereby stimulating the resolution of inflammation, while promoting tissue regeneration.[8,22] On the other hand, 17-HDHA can be metabolized to 17-oxo-docosahexaenoic acid (17-oxo-DHA, **3**), which may limit the formation of SPMs. Insight into its protein interaction partners in human immune cells would be of great benefit in obtaining a better molecular understanding of the biological role and metabolism of 17-HDHA.

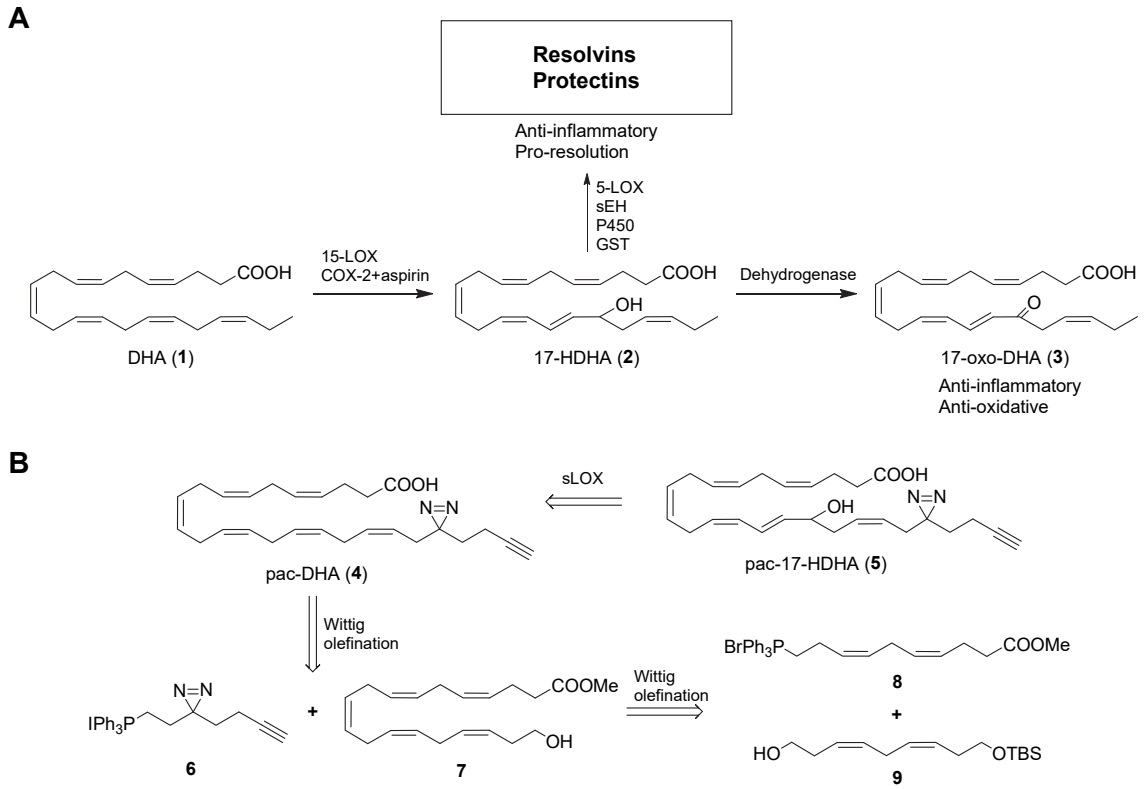

Scheme 1 | Oxidative metabolism of DHA (1) and synthetic strategy of photoaffinity probes 4 and 5. (A) Metabolic pathway of DHA to 17-oxo-DHA, resolvins and protectins. **(B)** Structures of photoaffinity-click (pac-)probes based on DHA (**1**) and 17-HDHA (**2**). The synthetic strategy included the use of soybean lipoxygenase (sLOX) to introduce the hydroxyl and the use of Wittig reactions to join building blocks **6**, **8** and **9**.

Lipid photoaffinity probes have been successfully used to map protein-lipid interactions on a global scale in their native environment.[23] Bioorthogonal photoaffinity lipid probes consist of a lipid modified with a photoreactive group and bioorthogonal ligation handle.[24] The photoreactive group is activated by irradiation with light, generating a reactive species that may form a covalent and irreversible bond with the interacting protein. The ligation handle is used to attach a reporter group via bioorthogonal chemistry, which allows for visualization or isolation of the probe-bound protein in a complex biological sample. This affinity-based protein profiling (AfBPP) approach has been reported for multiple lipid classes including phospholipids,[25,26] fatty acids,[23,27] sphingolipids[28,29] and sterols,[24,30] but has not been applied to omega-3 PUFAs, arguably due to the synthetic challenges associated with their preparation.[31]

An important drawback of photoreactive lipid-based probes is their inherent high lipophilicity and nonspecific binding to proteins. Significant overlap between protein targets of lipid probes has been documented, making it difficult to assign specific interaction partners to a given probe and to study their biological role.[32,33] Competition experiments with non-labeled lipids have been applied to identify specific binding partners, but were not always successful, possibly due to accumulation of both probe and competitor lipids in the cellular membrane.[34,35]

Here, the design, synthesis and application of a pair of complementary photoaffinity probes is described (**4** and **5**) based on the structure of DHA and 17-HDHA, respectively (Scheme 1B). The aim was to map the specific binding partners of 17-HDHA in primary human macrophages by comparative AfBPP, an approach capable of uncovering genuine, specific probe targets (Figure 1). Probe **5** retained the anti-inflammatory properties of the parent lipid in human M2 macrophages. Using chemical proteomics, specific protein binding partners of the probes were mapped. Prostaglandin reductase 1 (PTGR1) was identified and validated as a probe **5**-specific target. Subsequent biochemical studies revealed that PTGR1 oxidizes 17-HDHA into the anti-inflammatory 17-oxo-DHA in human macrophages. 17-oxo-DHA reduced the biosynthesis of the proinflammatory lipids in primary human neutrophils. These results demonstrate the potential of comparative photoaffinity protein profiling for the discovery of metabolic enzymes of bioactive lipids and highlight the power of chemical proteomics to uncover new biological insights.

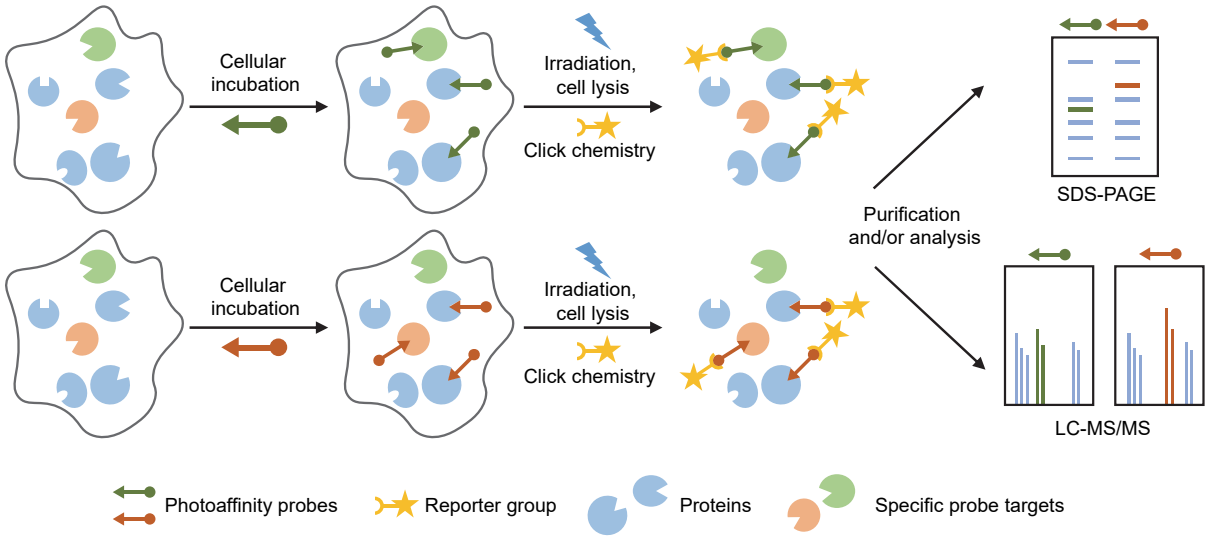

Figure 1 | Schematic overview of comparative AfBPP experiment. Two probes are used to identify all probe-interacting proteins. Then, probe-specific targets (green and red) can be identified after eliminating common (blue) probe targets.

Results

Design and synthesis of photoaffinity probes **4** and **5**

In the design of photoaffinity probes **4** and **5** (Scheme 1B) and to ensure they closely resemble the signaling lipids DHA and 17-HDHA, respectively, the polyunsaturated fatty acid scaffold was kept intact and the omega carbon was substituted with a diazirine- and alkyne-containing minimalistic bifunctional group.[36] Diazirines are small photoreactive groups with short reactive half-lives upon activation, thereby minimizing the interference and reducing non-specific labeling. The alkyne is the smallest bioorthogonal tag available and has similar physio-chemical properties to the alkyl chain of fatty acids.[37,38]

To synthesize the probes in an efficient manner, a chemoenzymatic approach was used. Probe **5** was produced by soybean lipoxygenase using probe **4** as substrate (Scheme 1B). Probe **4** was synthesized by combining two strategic building blocks, the minimalistic bifunctional photoreactive linker **6** and the polyunsaturated fatty acid scaffold (**7**), using a Wittig reaction. Building block **7** was generated by combining the two dienes **8** and **9**, also via a Wittig reaction. This synthetic strategy avoids the reduction of six skipped (non-conjugated) alkynes at the same time, which would lead to a complex mixture of partially hydrogenated products.[39] Moreover, this strategy did not require the assembly of large, skipped polyalkyne structures, which are inherently unstable.[40,41]

The synthesis of building block **6** started with reacting commercially available ethyl 3-oxobutanoate (**10**) with propargyl bromide using a protocol adapted from literature (Scheme 2).[36] Alkyne **11** was purified by fractional vacuum distillation and subsequently protected as a ketal by using ethylene glycol, followed by reduction of the ester with $LiAlH_4$. The resulting alcohol **12** was hydrolyzed under acidic conditions to form ketone **9**. This ketone was transformed into a diazirine in a three-step sequence. First, an imine was formed with saturated ammonia in methanol, after which reaction with hydroxylamine-*o*-sulfonic acid generated the diaziridine, which was oxidized with elemental iodine in methanol to form diazirine **14** in a yield of 37%. Alcohol **14** was halogenated using iodine in an Appel reaction to obtain compound **15**, after which the iodide was substituted with triphenylphosphine at 70 °C to form **6** in 73% yield over two steps.

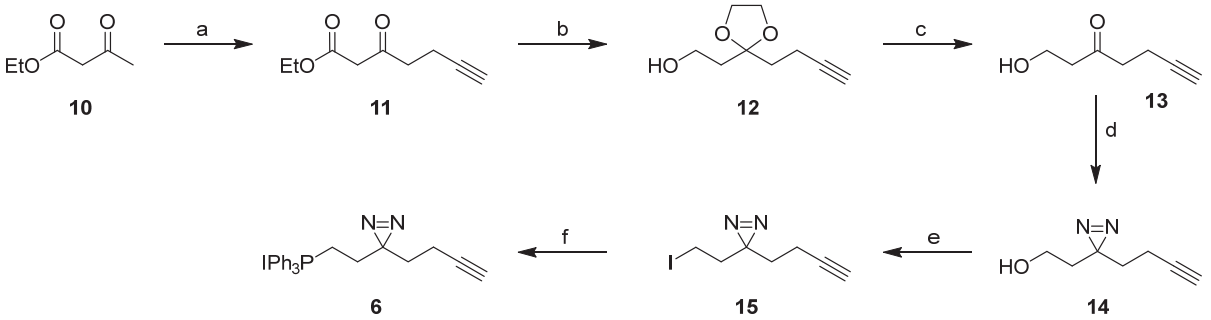

Scheme 2 | Synthesis of diazirine- and alkyne-containing building block 6. Reagents and conditions: (a) diisopropylamine, *n*-BuLi, THF, -78 °C to -40 °C, then **6**, propargyl bromide, -40 °C to 0 °C, 45%; (b) ethylene glycol, *p*-TsOH, triethyl orthoformate, 80 °C; then $LiAlH_4$, THF, 0 °C to rt, 94% over 2 steps; (c) acetone, H_2O, *p*-TsOH, 50 °C, 93%; (d) NH_3, hydroxylamine-*o*-sulfonic acid, MeOH, 0 °C to rt, then I_2, Et_3N, MeOH, 0 °C, 37%; (e) imidazole, I_2, PPh_3, DCM, 0 °C to rt, 73%; (f) PPh_3, ACN, 70 °C, quant.

The double bond system in building block **7** was assembled by joining fragments **8** and **9** (Scheme 3). To this end, butynol (**16**) was protected with a TBS group to afford alkyne **17** in 98% yield. This compound was deprotonated using *n*-butyllithium and reacted with paraformaldehyde to afford alcohol **18**, which was tosylated to obtain **19**. This intermediate was used without further purification for a copper(I)-mediated coupling to butynol to afford skipped alkyne **20** in 71% yield over three steps. The skipped alkyne was partially hydrogenated using a nickel boride catalyst to furnish alcohol **9** in 64% yield.

For fragment **8**, pentynoic acid (**21**) was protected by esterification in methanol to obtain **22**, which was reacted with sulfonate ester **19** in a second copper(I)-mediated coupling to afford skipped alkyne **23** (Scheme 2). Skipped alkyne **23** was partially hydrogenated to afford silylated **24**. The TBS group was removed using TBAF to afford alcohol **25**, which was halogenated to form **26**. This was then substituted with triphenylphosphine to afford phosphonium salt **8** in 43% yield from pentynoic acid.

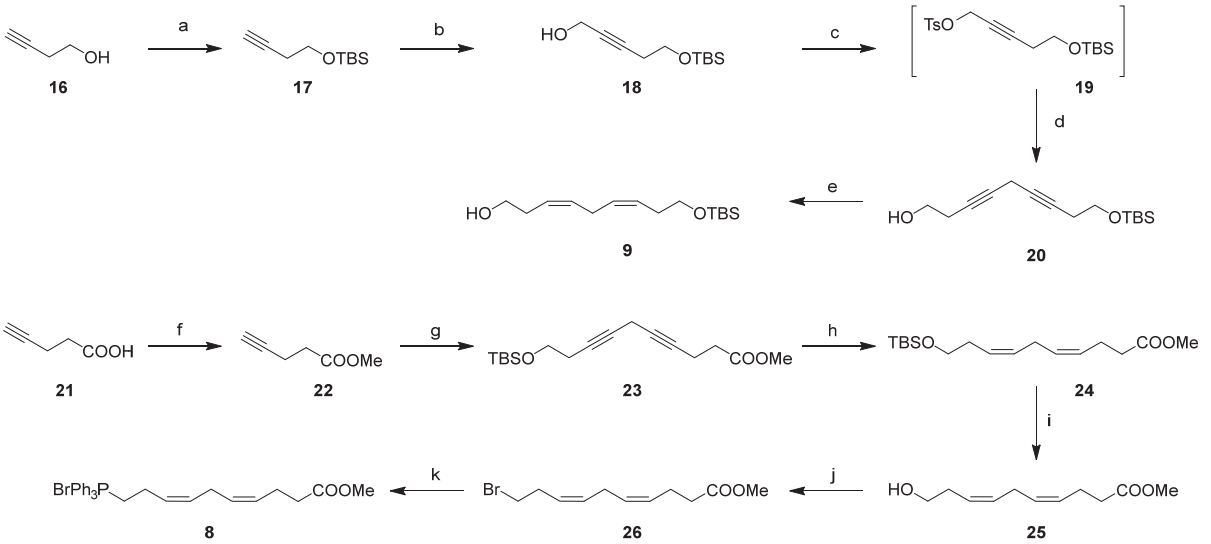

Scheme 3 | Synthesis of diene fragments 8 and 9. Reagents and conditions: (a) imidazole, TBSCl, DMF, 0 °C, 98%; (b) *n*-BuLi, paraformaldehyde, THF, -40 °C, 82%; (c) TsCl, KOH, Et_2O, 0 °C to rt; (d) CuI, NaI, Cs_2CO_3, but-3-yn-1-ol, DMF, 86%; (e) $Ni(OAc)_2 \cdot 4H_2O$, $NaBH_4$, ethylenediamine, EtOH, 64%; (f) $SOCl_2$, MeOH, 0 °C to rt, 92%; (g) **19**, CuI, NaI, Cs_2CO_3, DMF, 74%; (h) $Ni(OAc)_2 \cdot 4H_2O$, $NaBH_4$, ethylenediamine, EtOH, 89%; (i) TBAF, THF, 0 °C to rt, 71%; (j) CBr_4, PPh_3, DCM, -30 °C to 0 °C, quant.; (k) PPh_3, ACN, 92 °C, quant.

To join intermediates **8** and **9**, a Wittig reaction was performed by deprotonation of **8** to form ylid **27** using LiHMDS at reduced temperature, and addition of freshly prepared aldehyde **28** at -100 °C (Scheme 4). Alcohol **9** was oxidized using DMP to generate aldehyde **28** directly before use due to the instability of β,γ-unsaturated aldehydes.[42,43] This resulted in isolation of **29** with the newly generated alkene in *Z*-configuration in 57% yield, which was deprotected using TBAF to obtain alcohol **7** in 87% yield.

Building block **6** was installed in probe **4** by generating the final double bond using another Wittig reaction, for which alcohol **7** was oxidized with DMP, while phosphonium salt **6** was deprotonated with KO*t*Bu at reduced temperature. Higher temperatures or stronger bases resulted in loss of the diazirine. The freshly generated aldehyde **30** was added to the ylid at -105 °C which afforded methyl ester **31** in 38% yield after purification. The configuration of the last double bond was confirmed with NMR. Saponification of the ester yielded photoaffinity probe **4** in 83% yield.

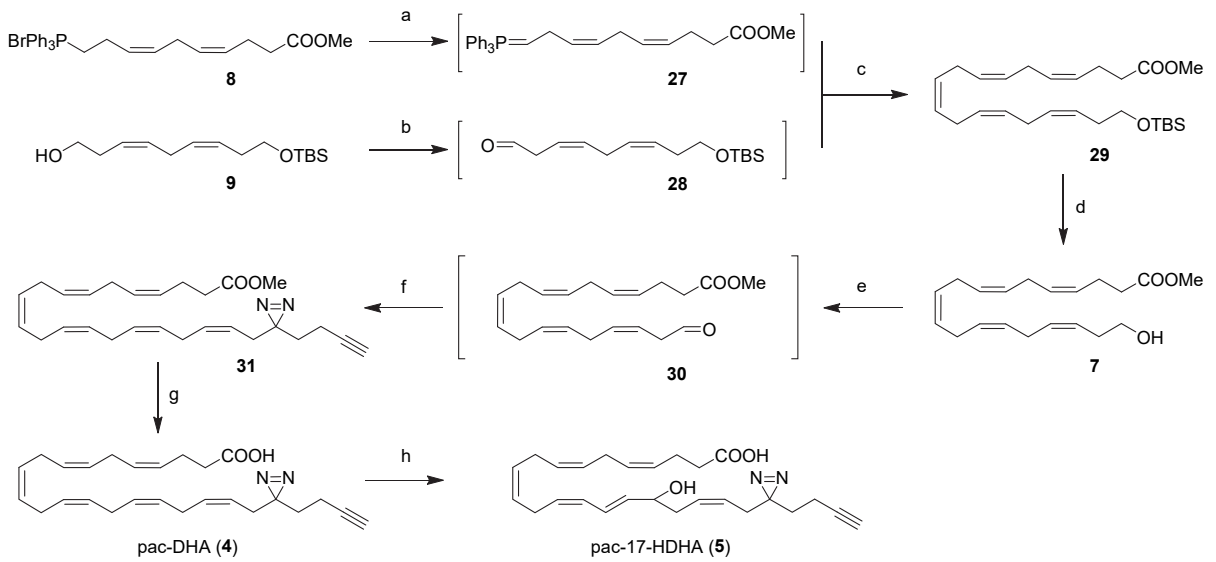

Scheme 4 | Formation of probes 4 and 5 by assembly of building blocks 6, 8 and 9. Reagents and conditions: (a) LiHMDS, THF, HPMA, -60 °C; (b) DMP, DCM, 0 °C to rt; (c) THF, HMPA, -100 °C to 0 °C, 57%; (d) TBAF, THF, 0 °C to rt, 87%; (e) DMP, DCM, 0 °C to rt; (f) **6**, *t*-BuOK, THF, -70 °C to -50 °C, then **30**, -105 °C to -30 °C, 38%; (g) LiOH, H_2O, THF, 0 °C to rt, 83%; (h) sLOX, borate buffer pH 12.0, 0 °C, then $NaBH_4$, then AcOH, 5%.

To generate photoaffinity-click (pac)-17-HDHA (**5**), commercially available soybean lipoxygenase (sLOX) was used, which catalyzes the oxidation of DHA (**1**) to 17-hydroperoxy-DHA, which can be reduced to 17-HDHA (**2**).[44,45] While DHA (**1**) was fully converted into 17-HDHA by sLOX using previously reported conditions,[46] this resulted in the complete loss of the diazirine when using probe **4** as substrate. To this end, the reaction conditions with probe **4** were optimized for enzyme loading, temperature and incubation time. This resulted in the formation of probe **5**, which could be obtained after high-performance liquid chromatography (HPLC) purification in sufficient quantities for cellular experiments, but not to determine the absolute configuration.

Mapping protein interaction partners of probe **4** and **5**

Probe **5** was tested in a cellular assay using primary human M2 macrophages to confirm it was biologically equivalent to 17-HDHA. M2 macrophages were differentiated from monocytes of healthy donors in the presence of macrophage colony-stimulating factor (M-CSF). Upon stimulation with Ca^{2+} ionophore, M2 macrophages rapidly synthesize the proinflammatory lipid 5-HETE from arachidonic acid (AA) by 5-lipoxygenase (Figure 2A). A liquid chromatography-mass spectrometry (LC-MS) method was developed to quantify 5-HETE and its precursor AA in these human macrophages. Upon pre-incubation with 17-HDHA lipid or probe **5**, conversion of AA into 5-HETE was reduced to the same extent by both molecules. Moreover, in primary human neutrophils also no loss in anti-inflammatory signaling was observed (Figure S1). These results indicate that the probe retains the anti-inflammatory signaling capacity of 17-HDHA and can be used to investigate the binding partners of its parent lipid.

Next, the protein interaction landscape of probe **5** in human M2 macrophages was investigated using two-step AfBPP. To identify specific targets of 17-HDHA, probe **4** was also used to map general, promiscuous lipid binding proteins. To this end, cells were incubated with probe **4** or **5** in serum-free medium for 30 min. Crosslinking was effected by UV-irradiation (λ = 350 nm, 10 min) using a CaproBox,[47] which irradiated the cells with simultaneous cooling at 4 °C to counteract the heat induced by the irradiation. Next, the cells were harvested, lysed and subjected to copper(I)-catalyzed azide-alkyne cycloaddition (CuAAC, "click"-reaction)[48] conditions utilizing Cy5-N_3 to enable the visualization of the probe-bound proteins by sodium dodecyl sulfate polyacrylamide gel electrophoresis (SDS-PAGE) analysis and in-gel fluorescence scanning (Figure 2B). This resulted in the visualization of many fluorescent bands for both probes, which were absent in the non-irradiated samples, demonstrating that the probes do not covalently interact with proteins without UV-irradiation. Although a large overlap in fluorescent bands was revealed after labeling by either probe **4** or **5**, there were also several probe-specific bands observed (Figure 2B).

To identify the probe-interacting proteins, the cell lysates were ligated to biotin-N_3 and a chemical proteomics experiment was performed. Briefly, the probe-labeled proteins were enriched using avidin-coated agarose beads, digested using trypsin and the resulting tryptic peptides analyzed by LC-MS. This resulted in the identification of 179 proteins after deselection based on identified unique peptides and appearance in the CRAPome.[49] Of these, 34 were significantly UV-enriched by probe **5** (Figure 2C/D, Table S1). To identify probe **5**-specific interacting proteins, the UV enrichment profiles of both probes were compared (Figure 2D, Table 1). Proteins which were previously identified as promiscuous lipid probe binders[33] are indicated in red. All promiscuous lipid probe binders, with the singular exception of voltage-dependent anion channel 2 (VDAC2), were equally enriched by both probes. This demonstrated that comparative AfBPP is capable of discovering genuine probe-specific interactions. Eight and ten proteins were specifically labeled by probe **4** and **5**, respectively.

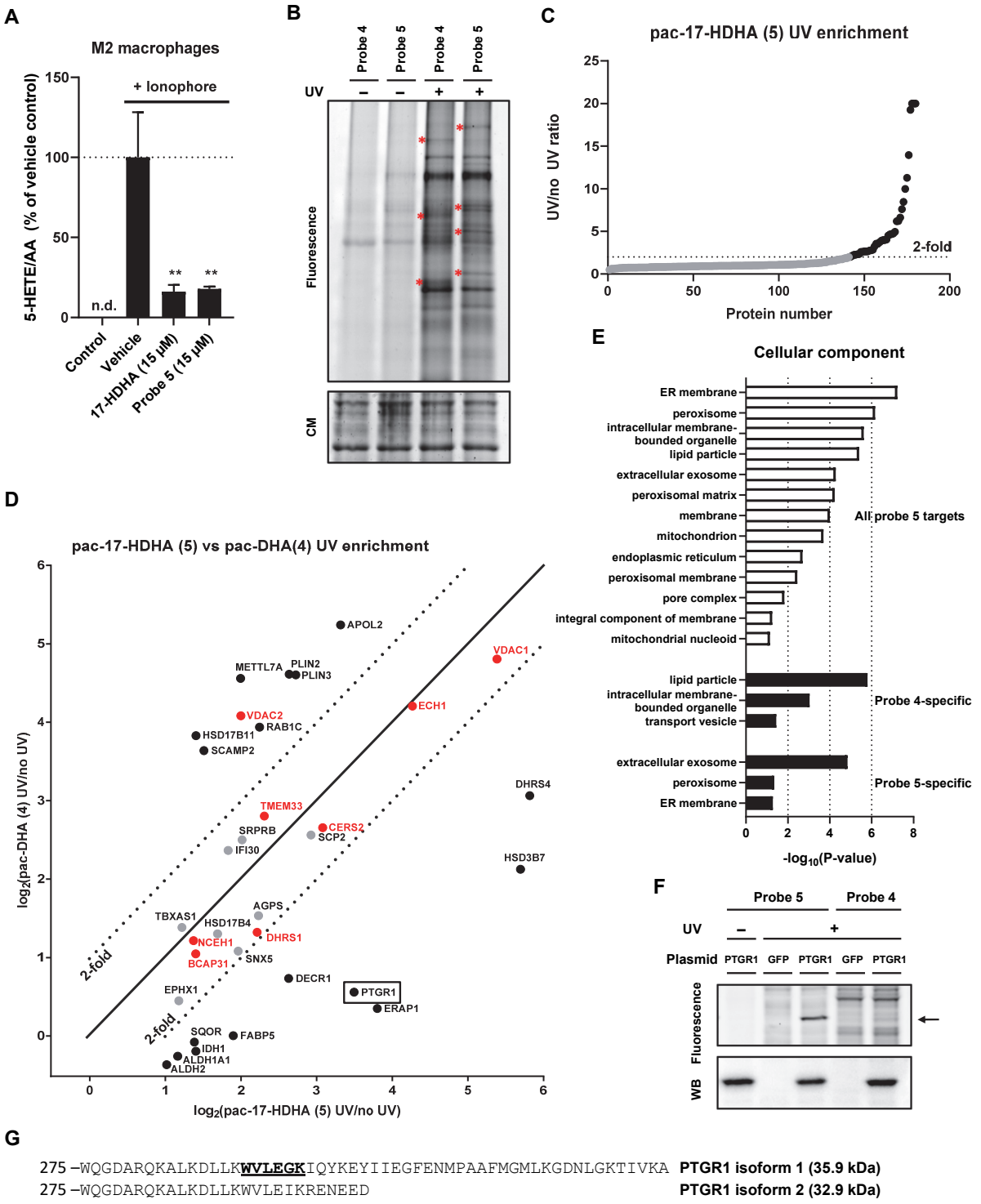

Figure 2 | Comparative ABPP in human M2 macrophages using pac-17-HDHA and pac-DHA. (A) 5-HETE/AA ratio (LC-MS/MS) produced by ionophore-stimulated M2 macrophages. Data represent means ± SD of representative donor (n = 3). ** $p < 0.01$ in comparison to ionophore-treated control using a one-way ANOVA with Dunnett's multiple comparisons correction. n.d.; not detected. **(B)** Probe targets of pac-17-HDHA (**5**) and pac-DHA (**4**) conjugated to Cy5-N_3 analyzed by SDS-PAGE and in-gel fluorescent scanning show UV-dependent and probe-specific labeling. Coomassie (CM) served as a protein loading control. Asterisks indicate probe-specific labeling. **(C)** Waterfall plot of proteins identified using probe **5** in M2 macrophages. **(D)** UV enrichment by probe **4** and probe **5** is shown and a 2-fold cutoff indicates probe-specific targets, promiscuous lipid probe binders[33] are indicated in red. **(E)** Cellular component analysis of probe **5**-interacting proteins by gene ontology (GO). **(F)** Gel-based AfBPP of GFP- or PTGR1-overexpressing HEK-293-T using probes **4** and **5**. Expression of PTGR1 was shown by anti-FLAG western blot. **(G)** PTGR1 amino acid sequence starting at W275. One of the identified tryptic peptides is indicated.

Gene ontology (GO) enrichment analysis revealed that the proteins significantly UV-enriched by probe **5** are mainly found in organelles in lipid metabolism, such as the endoplasmic reticulum and mitochondria. However, when the targets are narrowed down to probe-**5**-specific targets, the proteins are significantly associated with the extracellular exosomes gene ontology term (Figure 2E).[50] The probe **5**-specific targets are also predominantly involved in lipid metabolism (ALDH2/1A1, DECR1, DHRS4, HSD3B7, PTGR1) or transport (FABP5).

Table 1 | List of probe-specifically enriched targets of probe 5.

Uniprot accession	Gene name	Unique peptides	Description	Specific
Q9H2F3	HSD3B7	3	3 beta-hydroxysteroid dehydrogenase type 7	Probe **5**
Q9NZ08	ERAP1	20	Endoplasmic reticulum aminopeptidase 1	
Q14914	**PTGR1**	**11**	**Prostaglandin reductase 1**	
Q9BTZ2	DHRS4	10	Dehydrogenase/reductase SDR family member 4	
Q16698	DECR1	4	2,4-dienoyl-CoA reductase, mitochondrial	
Q01469	FABP5	2	Fatty acid-binding protein, epidermal	
O75874	IDH1	8	Isocitrate dehydrogenase [NADP], cytoplasmic	
Q9Y6N5	SQOR	6	Sulfide:quinone oxidoreductase, mitochondrial	
P00352	ALDH1A1	17	Retinal dehydrogenase 1	
P05091	ALDH2	16	Aldehyde dehydrogenase, mitochondrial	
Q92928	RAB1C	2	Putative Ras-related protein Rab-1C	Probe **4**
Q99541	PLIN2	11	Perilipin-2	
Q9BQE5	APOL2	4	Apolipoprotein L2	
O60664	PLIN3	2	Perilipin-3	
P45880	VDAC2	7	Voltage-dependent anion-selective channel protein 2	
O15127	SCAMP2	2	Secretory carrier-associated membrane protein 2	
Q8NBQ5	HSD17B11	2	Estradiol 17-beta-dehydrogenase 11	
Q9H8H3	METTL7A	2	Methyltransferase-like protein 7A	

Prostaglandin reductase 1 (PTGR1) is known for its role in inflammatory lipid metabolism and was therefore selected for further investigation.[51] PTGR1 (isoform 1, Figure 2G) expression is, for example, increased during inflammation and is involved in the resolution of inflammation through modulation of the HMGB1-miR522-3P-PTGR1 axis.[52] PTGR1 functions as 15-oxo-prostaglandin 13-reductase and acts on 15-oxo-PGE1 and 15-oxo-PGE2.[51,52] Furthermore, it catalyzes the conversion of the proinflammatory leukotriene B4 (LTB4) into its biologically less active metabolite, 12-oxo-LTB4, which is an initial and key step of metabolic inactivation of LTB4.[53] To validate PTGR1 as a specific target of probe **5**, a recombinant PTGR1-FLAG-tag fusion construct in a pcDNA3.1 plasmid was transfected in HEK-293-T cells. These cells and GFP-transfected control cells were subsequently subjected to gel-based AfBPP analysis with probe **4** and **5** (Figure 2F). Western blotting confirmed successful expression of PTGR1. In line with previous experiments, PTGR1 was labeled in a UV-dependent manner by probe **5**, but not by probe **4**, thereby confirming that PTGR1 is a specific target of probe **5**.

Biological role of PTGR1 in 17-HDHA metabolism

Since PTGR1 is capable of oxidizing the proinflammatory lipid LTB4, thereby converting the 12-hydroxyl group to form 12-oxo-LTB4,[51,54] it was hypothesized that by analogy PTGR1 may oxidize 17-HDHA into 17-oxo-DHA in human M2 macrophages. To this end, a targeted lipidomics method was developed to quantify 17-oxo-DHA in human cells. Upon incubation of M2 macrophages with 17-HDHA, the formation of 17-oxo-DHA could be detected in a concentration-dependent manner (Figure 3A). To investigate the role of PTGR1 in 17-HDHA metabolism, M2 macrophages were pre-incubated with two compounds with PTGR1 inhibitory activity. Indomethacin, better known as a COX-2 inhibitor, has a weak (IC_{50} 8.7 – 97.9 μM)[51,55] activity on PTGR1 (Figure 3E), whereas the anticancer compound licochalcone A is a potent, covalent inhibitor by covalently binding to C239.[56,57] Preincubation with indomethacin resulted in a relatively small reduction in the cellular levels of 17-oxo-DHA, whereas licochalcone A abolished 17-oxo-DHA formation (Figure 3B). Furthermore, 17-HDHA levels remained high upon addition of licochalcone A, which indicated a direct substrate-product relationship (Figure 3C). Of note, stimulation of M2 macrophages using calcium ionophore resulted in detection of formation of endogenous 17-HDHA and 17-oxo-DHA (Figure S2). Finally, it was investigated whether 17-oxo-DHA is instrumental in the 17-HDHA-induced inhibition of 5-HETE production. Therefore, the effect of 17-oxo-DHA on the activation of human macrophages and neutrophils was investigated. When primary immune cells were incubated with 17-oxo-DHA, a dose-dependent inhibition in the inflammatory response of M2 macrophages and neutrophils was observed as measured by the production of 5-HETE and LTB4. (Figure 3D, F and G).

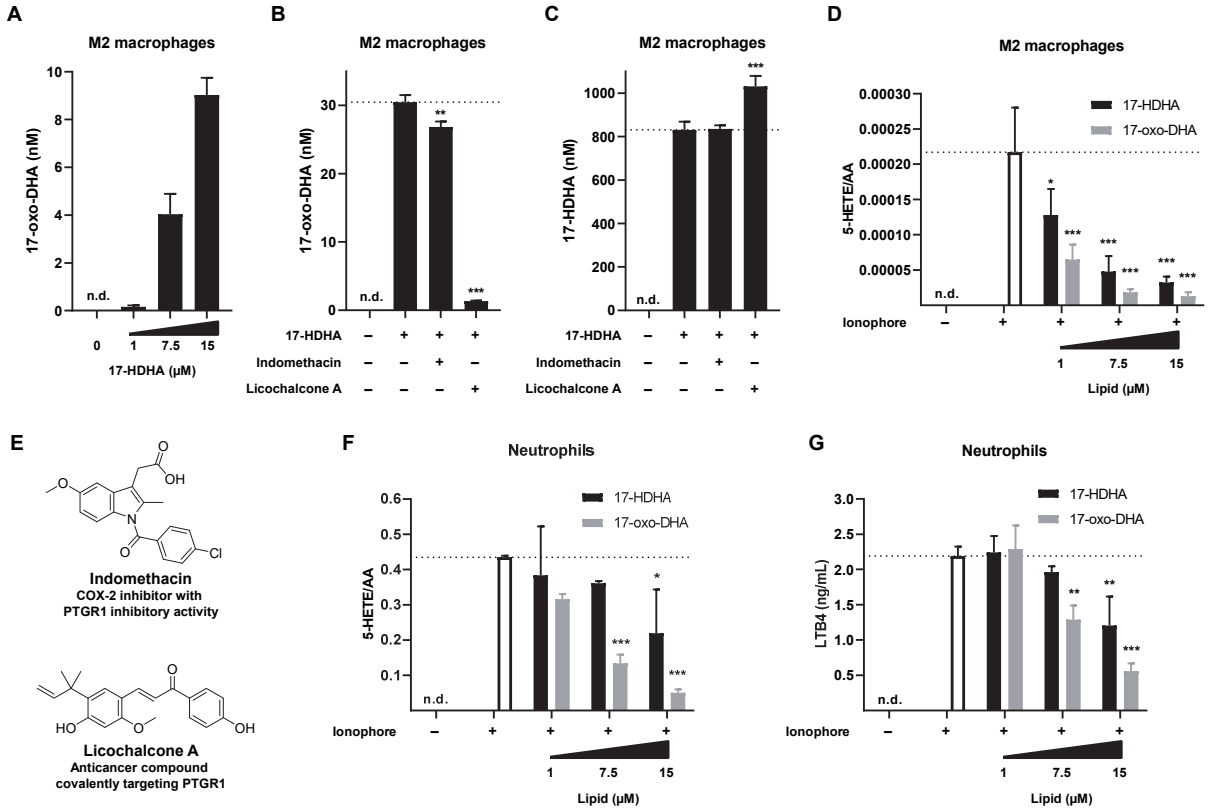

Figure 3 | Immune cells convert 17-HDHA into 17-oxo-DHA, which is reduced by inhibiting PTGR1. **(A)** 17-oxo-DHA produced by M2 macrophages. Cells were either pretreated for 2 h with 17-HDHA or vehicle control. **(B)** 17-oxo-DHA and **(C)** 17-HDHA measured in M2 macrophages show that inhibition of PTGR1 by indomethacin and licochalcone A reduces conversion of 17-HDHA to 17-oxo-DHA. Cells were pretreated for 30 min with 10 μM indomethacin, licochalcone A or vehicle before treatment with 17-HDHA (15 μM) or vehicle for 2 h. **(D)** 5-HETE/AA ratio (LC-MS/MS) produced by ionophore-stimulated M2 macrophages. Cells were either pretreated for 15 min with 17-HDHA, 17-oxo-DHA or vehicle control. **(E)** Structures of indomethacin and licochalcone A. **(F)** 5-HETE/AA ratio and **(G)** LTB4 levels (LC-MS/MS) produced by ionophore-stimulated neutrophils. Cells were either pretreated for 10 min with 17-HDHA, 17-oxo-DHA or vehicle control. Data represent means ±SD of representative donor (n = 2-3). * $p < 0.05$, ** $p < 0.01$, *** $p < 0.001$ in comparison to vehicle control (dotted line) using a one-way ANOVA with Dunnett's multiple comparisons correction. n.d.; not detected.

Discussion & Conclusion

Omega-3 fatty acids have well-established anti-inflammatory effects. Mechanistic studies indicate that the anti-inflammatory properties of omega-3 fatty acids are linked to their oxidative metabolism, but the molecular mode of action of the oxidative metabolites in human immune cells remains poorly understood.[1,2] In this chapter, a comparative chemical proteomic approach was developed using two complementary bifunctional photoreactive probes **4** and **5**, which were based on the scaffold of the polyunsaturated fatty acid DHA and its oxidative metabolite 17-HDHA. This allowed the identification of PTGR1 as an enzyme catalyzing the conversion of 17-HDHA into 17-oxo-DHA in human M2 macrophages. This finding is important, as it demonstrates that like lipoxygenase enzymes, PTGR1 is simultaneously metabolizing pro- and anti-inflammatory lipids. Macrophages are important players in both the initiation and resolution phase of inflammation and the metabolic network of immunomodulatory lipids needs to be uncovered to understood how this process is dysregulated in chronic inflammatory disease.

Previously, it was reported that 17-oxo-DHA is formed via COX-2-mediated oxidation of DHA, followed by a dehydrogenation step by an undetermined dehydrogenase enzyme.[58] 17-oxo-DHA acts as an anti-inflammatory lipid in leukocytes of COPD patients by inhibiting the NLRP3 inflammasome[59] and as a PPARα/γ dual agonist.[60] Moreover, it was shown to induce an anti-oxidant response through Nrf2 in mice[61] and by inhibiting ROS generation.[62] Here, it was discovered that 17-HDHA formed by 15-LOX metabolism is also used as a substrate for the formation of 17-oxo-DHA in human macrophages, which can be inhibited by two distinct inhibitors of PTGR1. It was also found that 17-oxo-DHA reduces the formation of the proinflammatory lipids 5-HETE and LTB4 in macrophages and neutrophils, thereby exerting anti-inflammatory effect. This suggests that 17-oxo-DHA could act as an inhibitor of 5-lipoxygenase, which is responsible for the production of 5-HETE and LTB4. Alternatively, it is conceivable that 17-oxo-DHA may indirectly modulate the activity of 5-lipoxygenase, for example, by reducing its expression or binding to 5-lipoxygenase activating protein (FLAP).[63]

Altogether, this study extends previous reports suggesting that PTGR1 serves as a metabolic hub that inactivates proinflammatory LTB4 and produces anti-inflammatory DHA derivatives, thereby modulating the cellular levels of these important signaling lipids that act in concert to affect the human macrophage-neutrophil axis. Finally, these results highlight the use of complementary bifunctional, photoreactive probes to identify specific protein interaction partners of promiscuous, lipophilic signaling molecules and also showcase the power of chemical proteomics in guiding the discovery of novel biological insights in primary human cells.

Experimental procedures

General

Lipids were purchased from Cayman Chemicals and stored as ethanolic stocks under argon at -80 °C. Reagents and inhibitors used for biochemical experiments were purchased from Cayman Chemicals or Sigma Aldrich unless otherwise specified and stored at -20 °C, except Cy5-N_3 (Figure S3), which was synthesized according to previously published procedures. Biotin-N_3 (Figure S3) was purchased from Bio-Connect Life Sciences.

Cloning

DNA oligos were purchased at Sigma Aldrich or Integrated DNA Technologies. Cloning reagents were from Thermo Fisher. Full-length cDNA encoding human PTGR1 or GFP was obtained from Source Bioscience. Expression constructs were generated by PCR amplification and restriction/ligation cloning into a pcDNA3.1 vector, in frame with a C-terminal FLAG tag. All plasmids were isolated from transformed XL10-Gold or DH10B competent cells (prepared using E. coli transformation buffer set, Zymo Research) using plasmid isolation kits following the supplier's protocol (Qiagen). All sequences were verified by Sanger sequencing (Macrogen).

HEK-293-T culture

HEK-293-T cells were cultured at 37 °C under 7% CO_2 in DMEM (D6546, Merck) containing phenol red, stable glutamine, 10% (v/v) New Born Calf Serum (Thermo Fisher) and penicillin and streptomycin (200 µg/mL each, Duchefa). Cells were passaged twice a week at 80-90% confluence by resuspension in fresh medium. Cell lines were purchased from ATCC and were tested regularly for mycoplasma contamination. Cultures were discarded after 2-3 months of use.

Transfection of HEK-293-T cells

GFP- or PTGR1-overexpressing HEK-293-T cells were generated by seeding HEK-293-T cells on 12-well plates (4.0×10^4 cells/cm^2) 24 h before transfection. Culture medium was then aspirated and replaced with 400 µL fresh medium. A 3:1 (m/m) mixture of polyethylenimine (PEI) (1.875 µg/well) and plasmid DNA (0.625 µg/well) was prepared in serum-free culture medium (100 µL) and incubated for 15 min at rt. Transfection was performed by dropwise addition of the PEI/DNA mix to the cells. After 24 h, medium was refreshed. Cells were used 48 h post-transfection.

Gel-based AfBPP of HEK-293-T cells

Confluent HEK-293-T cells on 12-well plates were treated with probe as follows: Growth medium was aspirated, the cells were washed with PBS (0.5 mL) and a solution of pac-DHA (**4**) or pac-17-HDHA (**5**) (10 µM from 10 mM ethanolic stock) in serum-free DMEM supplemented with 0.1% delipidated BSA (0.5 mL) was added. The cells were incubated for 30 min at 37 °C after which the medium was aspirated and the cells were irradiated ("UV") in 1 mL ice-cold PBS using a Caprobox™ (10 min, 4 °C, 350 nm) or exposed to ambient light ("No UV"). The cells were harvested by pipetting and pelleted by centrifugation (1,000 *g*, 10 min, 4 °C). The supernatant was removed and the cells were lysed by resuspension in lysis buffer (250 mM sucrose, 20 mM HEPES pH 7.5, 1 mM $MgCl_2$) and sonication in a bath sonicator (0 °C, 10 s). Protein concentration was measured by Qubit™ assay (Invitrogen) and the samples were adjusted to 1.5 mg/mL and a volume of 100 µL, after which the samples were treated with 10.95 µL click mix (5.5 µL aq. 25 mM $CuSO_4$, 3.25 µL aq. 250 mM NaAsc, 1.1 µL 25 mM THPTA in DMSO, 1.1 µL 0.9 mM Cy5-N_3 in DMSO) and left at rt for 1 h. Samples were then quenched by addition of 4X Laemmli buffer, boiled (5 min, 95 °C) and resolved by SDS-PAGE (10% acrylamide gel, ±80 min, 180 V) along with protein marker (PageRuler™ Plus, Thermo Fisher). In-gel fluorescence was measured in the Cy3- and Cy5-channel (Chemidoc™ MP, Bio-Rad).

Proteins were then transferred to a 0.2 µm polyvinylidene difluoride membrane by Trans-Blot Turbo™ Transfer system (Bio-Rad). Membranes were washed with TBS (50 mM Tris pH 7.5, 150 mM NaCl) and blocked with 5% (w/v) milk in TBS-T (50 mM Tris pH 7.5, 150 mM NaCl, 0.05% (w/v) Tween-20) for 1 h at rt. Membranes were then incubated with primary antibody mouse-anti-FLAG (F3156, Merck, 1:2,000 in 5% (w/v) BSA in TBS-T, 1 h, rt), washed three times with TBS-T, incubated with secondary goat-anti-mouse-HRP (sc-2005, Santa Cruz Biotechnologies, 1:5,000 in 5% (w/v) BSA in TBS-T, 1 h, rt) and washed three times with TBS-T and once with TBS. Luminol development solution (10 mL of 1.4 mM luminol in 100 mM Tris pH 8.8 + 100 µL of 6.7 mM *p*-coumaric acid in DMSO + 3 µL of 30% (v/v) H_2O_2) was added and chemiluminescence was detected on ChemiDoc™ MP (Bio-Rad) in the chemiluminescence channel and colorimetric channel for the protein marker.

Macrophage and neutrophil isolation

This study was approved by the local medical ethical committee of the LUMC (METC), and written informed consent was given by all donors. Neutrophils were isolated from fresh 50 mL EDTA blood containers via DextranT500 sedimentation (Pharmacosmos). The upper layer was collected, followed by Ficoll density gradient separation. The remainder of the erythrocytes was removed by hypotonic lysis. Purity was checked by FACS (LSRIII, BD Biosciences) by staining the cells with CD3-AF700 (clone UCHT1)/CD15-APC (clone HI98)/CD16-PE (clone 3G8)/CD19-FITC (clone HIB19) and was typically above 97%. Isolated neutrophils were resuspended in Dulbecco's phosphate-buffered saline (DPBS) with $MgCl_2$ and $CaCl_2$ (D8662, Merck). Human peripheral blood mononuclear cells (PBMCs) were isolated by Ficoll density gradient from healthy donor buffy coats (Sanquin). Blood monocytes were isolated by positive selection from PBMCs using MACS CD14 Microbeads (Miltenyi Biotec) and purity was checked by FACS (LSRIII, BD Biosciences), by staining the cells with CD14-PE (clone MφP9). Purity was typical above >99%. Monocytes were differentiated for seven days in RPMI 1640 medium (Gibco) containing 8% FCS, 100 U/mL penicillin and streptomycin, 2 mM Glutamax (Thermo Fisher) and 50 ng/mL M-CSF (R&D Systems). 1/3rd of the medium was replenished containing 150 ng/mL M-CSF on day three and five. Phenotype was checked before experiments by visual inspection by assessing the typical morphology of M-CSF-treated monocyte-derived macrophages (elongated and spindle-like). Moreover, phenotype was also confirmed by performing IL-12 OptEIA (BD Biosciences), IL-10 PeliPair reagent set (Sanquin), and TNFα OptEIA (BD Biosciences) ELISA on supernatant of cells stimulated for 24 h with 10 ng/mL LPS (Merck). M-CSF-treated monocyte-derived macrophages secreted low IL-12 and TNFα and high IL-10 levels.

M-CSF-treated monocyte-derived macrophages (M2 macrophages) were harvested using Accutase (Merck) and for lipidomics experiments 2.5×10^5 cells were seeded in 24-well plates in 250 µL medium. All experiments were performed in phenol red-free RPMI 1640 medium (Gibco), supplemented with 0.1% (w/v) delipidated BSA (Merck), 100 U/mL penicillin and streptomycin, and 2 mM Glutamax. For lipidomics experiments, cells were pretreated with indicated amounts of 17(S)-HDHA (Cayman Chemicals) or vehicle, HPLC grade ethanol (Fischer Scientific), and indicated amount of inhibitor (Merck) or vehicle, 0.02% HPLC grade DMSO. Stimulation of both macrophages and neutrophils was done using 4 µM calcium ionophore A23178 (Merck) for 10 min.

Lipid isolation and LC-MS/MS

After treatment, cells and supernatant were quenched using three volumes of MeOH (Honeywell, 349661L) and internal standard mix containing known concentrations of three internal standards: 5 ng/mL DHA-d5, 500 pg/mL LTB4-d4 and 500 pg/mL 15(S)-HETE-d8 (Cayman Chemicals) for subsequent quantification. All samples were stored at -80 °C under argon until analysis. Quenched samples were centrifuged (20,000 *g*, 5 min) and the supernatant was transferred into an autosampler vial containing an equal volume of H_2O (Honeywell) before LC-MS/MS analysis, which was carried out as previously published.[64] The MS method was slightly adapted: it was extended with a MRM for 17-oxo-DHA (341 / 111). Lipid measurements were performed using a QTrap 6500 mass spectrometer in negative ESI mode (Sciex), coupled to a LC system employing LC-30AD pumps, a SIL-30AC auto sampler, and a CTO-20AC column oven (Shimadzu). A Kinetex C18 50 × 2.1 mm, 1.7 µm column

combined with a C8 precolumn (Phenomenex) was used and kept at 50 °C. A gradient of water and methanol with 0.01% acetic acid was used. The injection volume was 40 µL and a flow rate of 400 µL/min was used. MRM transitions used to identify LM were based on previous work by the group of M. Giera.[64] Peaks were integrated with manual supervision and retention time corrected to corresponding IS (RRT) with MultiQuant™ 2.1 (Sciex). Only peaks with a signal to noise (S/N) >10 were quantified. Calibration curves were constructed using authentic synthetic standards 17-HDHA, 17-oxo-DHA, AA, DHA, LTB4, 5-HETE, LTD4, LTE4, 15(S)-HETE-d8, LTB4-d4 and DHA-d5 which were purchased from Cayman Chemicals.

AfBPP of M2 macrophages

M-CSF-treated monocyte-derived macrophages were plated on 6-well plates. The following day, they were washed with PBS (1 mL) and probe incubation was started by adding pac-DHA or pac-17-HDHA (10 µM from 10 mM ethanolic stock) in serum-free RPMI supplemented with 0.1% (w/v) delipidated BSA (1 mL). The cells were incubated for 30 min at 37 °C after which the medium was aspirated and replaced with ice-cold PBS. The cells were irradiated using a Caprobox™ (10 min, 4 °C, 350 nm, "UV") or exposed to ambient light (10 min, 4 °C, "No UV"). The PBS was collected in tubes and floating cells were spun down (1,000 *g*, 10 min, 4 °C) and the PBS was aspirated. The cells in the wells were lysed with lysis buffer (250 µL, 250 mM sucrose, 1X protease inhibitor cocktail (Roche), 20 mM HEPES pH 7.5, 1 mM $MgCl_2$). The material was harvested by scraping and combined with the cell pellet. This was sonicated (Branson Sonifier probe sonicator, 10 x 1 s pulses, 10% amplitude). Protein concentration was measured by Qubit™ assay (Invitrogen) and the samples were adjusted to 0.5 mg/mL and a volume of 440 µL, of which 40 µL was reserved for gel analysis. For gel analysis, the 40 µL lysate was treated with freshly prepared click mix (4.37 µL per sample: 2.19 µL aq. 25 mM $CuSO_4$, 1.3 µL aq. 250 mM NaAsc, 0.44 µL 25 mM THPTA in DMSO, 0.44 µL 0.9 mM Cy5-N_3 in DMSO) and left at rt for 1 h in the dark. Samples were then quenched by addition of 4X Laemmli buffer, boiled (5 min, 95 °C) and resolved by SDS-PAGE (10% acrylamide gel, ±80 min, 180 V) along with protein marker (PageRuler™ Plus, Thermo Fisher). In-gel fluorescence was measured in the Cy3- and Cy5-channel (Chemidoc™ MP, Bio-Rad) and gels were stained with Coomassie after scanning.

Mass spectrometric analysis of tryptic peptides, identification and quantification

The pulldown experiment is performed as earlier described, with minor adjustments.[65,66] The lysates (400 µL) were subjected to a click reaction with freshly prepared click mix (43.7 µL per sample: 21.9 µL aq. 25 mM $CuSO_4$, 13 µL aq. 250 mM NaAsc, 4.4 µL 25 mM THPTA in DMSO, 4.4 µL 2.25 mM biotin-N_3 in DMSO) at rt for 1 h. Proteins were precipitated by addition of HEPES buffer (50 µL, 50 mM, pH 7.5), MeOH (666 µL), $CHCl_3$ (166 µL) and MilliQ (150 µL), vortexing after each addition. After spinning down (1,500 *g*, 10 min) the upper and lower layer were aspirated and the protein pellet was resuspended in MeOH (600 µL) by sonication (Branson Sonifier probe sonicator, 10 x 0.5 s pulses, 10% amplitude). The proteins were spun down (20,000 *g*, 5 min) and the MeOH was aspirated. The proteins were then redissolved in 6 M urea (500 µL) with 25 mM NH_4HCO_3 for 15 min, followed by reduction (65 °C, 15 min, 800 rpm shaking) with DTT (5 µL, 1 M). The samples were allowed to reach rt and proteins were alkylated (30 min) with IAA (40 µL, 0.5 M) in the dark. 140 µL SDS (10% w/v) was added and the samples were spun down (1,000 *g*, 5 min). They were transferred to 5 mL PBS containing 50 µL avidin agarose resin (Pierce, 100 µL of a 50% slurry, prewashed twice with 6 mL PBS + 0.5% SDS and once with 6 mL PBS) and incubated for 2 h while rotating. The beads were then spun down (2,000 *g*, 2 min) and washed (3 x PBS + 0.25% SDS, 2 x PBS, 1 x MilliQ). The beads were resuspended in digestion buffer (250 µL, 100 mM Tris pH 7.8, 100 mM NaCl, 1 mM $CaCl_2$, 2% (v/v) acetonitrile, sequencing grade trypsin (Promega, 0.25 µg)) and transferred to low-binding tubes (Sarstedt) and incubated while shaking overnight (16 h, 37 °C, 1,000 rpm). Trypsin was quenched with 12.5 µL formic acid (LC-MS grade) and the beads were then filtered off over a Bio-Spin column (BioRad, 400 *g*, 5 min), collecting the flow-through in a new 2 mL tube. Samples were added on C18 stagetips[67] (preconditioned with 50 µL MeOH, then 50 µL of 0.5% (v/v) formic acid in 80% (v/v) acetonitrile/MilliQ (solution B) and then 50 µL 0.5% (v/v) formic acid in MilliQ (solution A) by centrifugation (600 *g*, 2 min)). The peptides were washed with

solution A (100 µL, 800 *g*, 3 min) and eluted into new low-binding tubes using solution B (100 µL, 800 *g*, 3 min). Samples were concentrated using an Eppendorf speedvac (Eppendorf Concentrator Plus 5301) and redissolved in LC-MS solution (30 µL per sample: 28.5 µL MilliQ, 2.85 µL acetonitrile, 0.095 µL formic acid, 600 fmol yeast enolase peptide digest (Waters, 186002325)).

Samples were measured using a NanoACQUITY UPLC System coupled to a SYNAPT G2-Si high definition mass spectrometer (Waters). The peptides were separated using an analytical column (HSS-T3 C18 1.8 µm, 75 µm x 250 mm, Waters) with a concave gradient (5 to 40% acetonitrile in H_2O with 0.1% formic acid). [Glu^1]-fibrinopeptide B was used as lock mass. Mass spectra were acquired using the $UDMS^e$ method. The mass range was set from 50 to 2,000 Da with a scan time of 0.6 seconds in positive, resolution mode. The collision energy was set to 4 V in the trap cell for low-energy MS mode. For the elevated energy scan, the transfer cell collision energy was ramped using drift-time-specific collision energies. The lock mass is sampled every 30 seconds. For raw data processing, Progenesis QI for proteomics was used with the following parameters to search the human proteome from Uniprot (Table S1). Albumin was not included in the analysis of probe targets.

Table S1 | Parameters used for Progenesis QI.

Parameter	Value
Lock mass *m*/*z* value	785.8426
Low energy threshold	150 counts
Elevated energy threshold	30 counts
Digest reagent	Trypsin
Missed cleavages	Max 2
Modifications	Fixed carbamidomethyl C, variable oxidation M
FDR less than	1%
Minimum fragments/peptide	2
Minimum fragments/protein	5
Minimum peptides/protein	1
Minimum peptide score for quantification	5.5
Identified ion charges for quantification	$2/3/4/5/6/7^+$

Statistical analysis

Unless otherwise noted, all data represent means ± SD. Statistical significance was determined using Student's t-tests (two-tailed, unpaired) or ANOVA with Dunnett's or Tukey's multiple comparisons correction. *** $p < 0.001$; ** $p < 0.01$; * $p < 0.05$; n.s. if $p > 0.05$. All statistical analysis was conducted using Graphpad Prism 8.1.1 or Microsoft Excel.

Synthesis

General remarks

Dry solvents were prepared by storage on activated 4 Å molecular sieves for at least 24 hours. The reactions were performed under an inert atmosphere of nitrogen gas unless stated otherwise. All reagents were purchased from Alfa Aesar, Sigma Aldrich/Merck or Acros and used without further purification. Flash column chromatography was performed using SiliCycle silica gel type SiliaFlash P60 (230-400 mesh). TLC analysis was performed on Merck silica gel 60/Kieselguhr F254, 0.25 mm. Compounds were visualized using $KMnO_4$ stain (K_2CO_3 (40 g), $KMnO_4$ (6 g), and water (600 mL)). ^{1}H NMR and ^{13}C NMR spectra were recorded on a Bruker AV-400 (400 MHz) or AV-500 (500 MHz) spectrometer. Chemical shift values are reported in ppm relative to the tetramethylsilane signal for ^{1}H NMR (δ = 0 ppm) and relative to the solvent signal of $CDCl_3$ for ^{13}C NMR (δ = 77.16 ppm). Data are reported as follows: Chemical shifts (δ), multiplicity (s = singlet, d = doublet, dd = doublet of doublets, ddt = doublet of doublet of triplets, td = triplet of doublets, t = triplet, q = quartet, p = pentet, bs = broad singlet, m = multiplet), coupling constants *J* (Hz), and integration. High resolution mass spectra (HRMS) were recorded by direct injection on a q-TOF mass spectrometer (Synapt G2-SI) equipped with an electrospray ion source in positive mode with Leu-enkephalin (m/z = 556.2771) as an internal lock mass. The instrument was calibrated prior to measurement using the MS/MS spectrum of [Glu^1]-fibrinopeptide B.

Preparative HPLC separations were performed with an Agilent Technologies 1200 series HPLC system using a Gemini column (5 µm C18, pore size: 100 Å, 250 x 10.0 mm) or Nucleodur column (5 µm C18, pore size: 110 Å, 250 x 10.0 mm) using a specified linear gradient (Gradient of solvent B in solvent A in 12 min, flow rate of 5 mL/min, detection at 210 - 600 nm by a diode array and Agilent 6130 series quadrupole mass detector, solvent A: 0.2% (v/v) TFA in H_2O, solvent B: acetonitrile). Analytical LC-MS was performed using a C18 column (50 x 4.6 mm, 3 µm; Nucleodur Gravity, Macherey-Nagel) connected to a Vanquish UHPLC system (Thermo Scientific) with a Vanquish Diode Array detector (Thermo Scientific) coupled to a LCQ™ Fleet (Thermo Scientific) via electrospray ionization (ESI). Acetonitrile and water containing TFA (0.1%) were used for chromatographic separation using an indicated gradient.

Fragmentation of pac-17-HDHA (**5**) was done after reduction of the double bonds, as LC-MS/MS fragmentation in negative mode was not successful, possibly due to activation of the diazirine during tandem MS. Pac-17-HDHA (**5**) was analyzed by complete hydrogenation of an analytical sample (50 nmol) in EtOH (1 mL) using catalytic PtO_2 and hydrogen gas, followed by the filtration of the catalyst by cotton, removal of the solvent under a stream of N_2 gas and redissolving in 100 µL acetonitrile, injecting 10 µL on a C18 column (50 x 4.6 mm, 3 µm; Gemini) connected to a Agilent Technologies 1260 Infinity system and eluting it with acetonitrile/H_2O (70:30) with 10 mM NH_4OAc onto a 6120 Quadrupole LC/MS (Agilent Technologies) equipped with an electrospray ion source in positive mode (source voltage 4 kV, sheath gas flow 10, capillary temperature 623 K).

Ethyl 3-oxohept-6-ynoate (11)

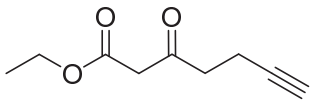

Freshly distilled diisopropylamine (20.43 mL, 143 mmol) was dissolved in dry THF (60 mL) and cooled to -78 °C. *n*-BuLi (1.4 M in hexane, 102 mL, 143 mmol) was added dropwise and the reaction was stirred for 15 min. The mixture was allowed to reach -40 °C after which ethyl 3-oxobutanoate (8.23 mL, 65.2 mmol) in dry THF (40 mL) was added dropwise. After 30 min of stirring, propargyl bromide (80 wt.% in toluene, 7.02 mL, 65.2 mmol) was added dropwise after which the reaction was allowed to reach 0 °C. After 1.5 h of stirring, it was quenched with 0.5 M aq. HCl (200 mL) and diluted with Et_2O (200 mL). The organic layer was collected and the aq. layer extracted with Et_2O (200 mL). The combined organic layers were washed with brine (100 mL), dried over $MgSO_4$, filtered and concentrated under reduced pressure to afford a dark brown oil, which was distilled (105-110 °C, 6.8 mmHg) to afford the title compound as a clear oil (4.943 g, 29.4 mmol, 45%). R_f = 0.60 (EtOAc/pentane = 1:4); ^{1}H NMR (400 MHz, $CDCl_3$) δ 4.20 (q, *J* = 7.1 Hz, 2H), 3.48 (s, 2H), 2.82 (t, *J* = 7.2 Hz, 2H), 2.48 (td, *J* = 7.2, 2.7 Hz, 2H), 1.98 (t, *J* = 2.7 Hz, 1H), 1.29 (t, *J* = 7.1 Hz, 3H); ^{13}C NMR (101 MHz, $CDCl_3$) δ 200.63, 166.95, 82.59, 69.05, 61.51, 49.23, 41.63, 14.13, 12.84. Spectra were consistent with previously reported data.[68]

2-(2-(But-3-yn-1-yl)-1,3-dioxolan-2-yl)ethan-1-ol (12)

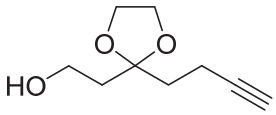

In a microwave vial, ketone **11** (0.8619 g, 5.12 mmol), ethylene glycol (2.143 mL, 38.4 mmol), *p*-TsOH·$2H_2O$ (0.049 g, 0.256 mmol) and triethyl orthoformate (2.56 mL, 15.37 mmol) were added, the vial was sealed and the reaction was stirred at 80 °C for 1.5 h. The mixture was diluted with Et_2O (5 mL) and quenched with sat. aq. $NaHCO_3$ (5 mL). It was then diluted with Et_2O (100 mL) and sat. aq. $NaHCO_3$ (100 mL). The layers were separated and the organic layer washed with brine (100 mL), dried over Na_2SO_4 and concentrated under reduced pressure to afford crude ethyl 2-(2-(but-3-yn-1-yl)-1,3-dioxolan-2-yl)acetate. The residue was diluted with dry THF (20 mL) and added dropwise to a cold (0 °C) mixture of $LiAlH_4$ (0.389 g, 10.24 mmol) and dry THF (20 mL). The reaction was allowed to reach rt and after 0.5 h it was cooled to 0 °C and quenched with EtOAc (5 mL). After 15 min, 10% (w/v) aq. Rochelle's salt (40 mL) was added and the mixture was allowed to reach rt overnight. The mixture was then diluted with brine (40 mL) and extracted with Et_2O (5 x 40 mL). The combined organic layers were washed with brine (100 mL), dried over Na_2SO_4, filtered, concentrated under reduced pressure and filtered over a plug of silica with EtOAc/pentane (1:1) to afford the title compound as a yellow oil (0.8204 g, 4.82 mmol, 94%). R_f = 0.63 (EtOAc); ^{1}H NMR (400 MHz, $CDCl_3$) δ 4.06 – 3.93 (m, 4H), 3.76 (q, *J* = 5.4 Hz, 2H), 2.72 (t, *J* = 5.5 Hz, 1H), 2.32 – 2.24 (m, 2H), 1.99 – 1.91 (m, 5H); ^{13}C NMR (101 MHz, $CDCl_3$) δ 111.12, 84.04, 68.36, 65.03, 58.76, 38.35, 35.99, 13.22. Spectra were consistent with previously reported data.[36]

1-Hydroxyhept-6-yn-3-one (13)

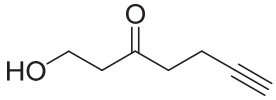

To a solution of ketal **12** (0.8204 g, 4.82 mmol) in acetone (19 mL) and water (1 mL) was added *p*-TsOH·$2H_2O$ (0.229 g, 1.205 mmol) and the reaction was stirred for 1 h at 50 °C. It was quenched with sat. aq. $NaHCO_3$ (50 mL) and diluted with EtOAc (50 mL). The aq. layer was separated and extracted with EtOAc (50 mL). The combined organic layers were washed with brine (50 mL), dried over $MgSO_4$, filtered, concentrated under reduced pressure and purified by column chromatography (EtOAc/pentane = 1:2 to 1:1) to afford the title compound as a yellow oil (0.565 g, 4.48 mmol, 93%). R_f = 0.62 (EtOAc); ^{1}H NMR (400 MHz, $CDCl_3$) δ 3.87 (t, *J* = 5.5 Hz, 2H), 2.76 – 2.68 (m, 5H), 2.46 (td, *J* = 7.1, 2.6 Hz, 2H), 1.98 (t, *J* = 2.7 Hz, 1H); ^{13}C NMR (101 MHz, $CDCl_3$) δ 209.03, 82.89, 68.95, 57.62, 44.68, 41.81, 12.78. Spectra were consistent with previously reported data.[36]

2-(3-(But-3-yn-1-yl)-3*H*-diazirin-3-yl)ethan-1-ol (14)

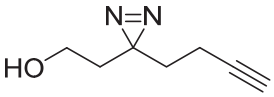

Ketone **13** (0.660 g, 5.23 mmol) was dried by coevaporation with toluene. It was dissolved in dry MeOH (15 mL) and cooled to 0 °C. NH_3 gas was bubbled through the solution for 30 min under stirring after which the reaction was stirred for 5 h. Then, hydroxylamine-*o*-sulfonic acid (0.887 g, 7.85 mmol) in dry MeOH (5 mL) was added dropwise and the reaction was allowed to reach rt overnight. It was filtered over celite and the filtrate was concentrated under reduced pressure. The residue was redissolved in dry MeOH (10 mL) and Et_3N (1.094 mL, 7.85 mmol) was added. The reaction was cooled to 0 °C and a sat. solution of I_2 in dry MeOH was added dropwise until the color persisted for 20 min (8 mL). The reaction was diluted with EtOAc (100 mL) and quenched with 1 M aq. $Na_2S_2O_3$ (100 mL). The layers were separated, the aq. layer was extracted with EtOAc (100 mL) and the combined organic layers were washed with 1 M aq. HCl (100 mL) and brine (100 mL), dried over $MgSO_4$, filtered and concentrated under reduced pressure. Column chromatography of the residue (EtOAc/pentane = 1:6 to 1:3) afforded the title compound as a yellow oil (0.2677 g, 1.937 mmol, 37%). R_f = 0.59 (EtOAc/pentane = 1:1); ^{1}H NMR (400 MHz, $CDCl_3$) δ 3.49 (t, *J* = 6.2 Hz, 2H), 2.10 – 2.01 (m, 2H), 1.99 (s, 1H), 1.77 – 1.65 (m, 4H); ^{13}C NMR (101 MHz, $CDCl_3$) δ 82.95, 69.34, 57.36, 35.56, 32.68, 26.72, 13.31; HRMS: Calculated for $[C_7H_{10}N_2O+H]^+$ 139.0866, found 139.0865.

3-(But-3-yn-1-yl)-3-(2-iodoethyl)-3*H*-diazirine (15)

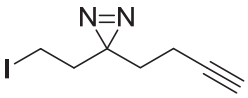

To a cooled (0 °C) solution of alcohol **14** (0.6617 g, 4.79 mmol) dry DCM (24 mL) was added imidazole (0.978 g, 14.37 mmol), I_2 (1.459 g, 5.75 mmol) and PPh_3 (1.382 g, 5.27 mmol). The reaction was allowed to reach rt and stirred for 3 h. It was cooled to 0 °C and quenched with 10% aq. $Na_2S_2O_3$ (50 mL) and diluted with DCM (100 mL). The aq. layer was isolated and extracted with DCM (100 mL) and the combined organic layers were dried over $MgSO_4$, filtered and concentrated under reduced pressure. Column chromatography of the residue (Et_2O/pentane = 1:49 to 1:16) afforded the title compound as a yellow liquid (0.8609 g, 3.47 mmol, 73%). R_f = 0.69 (EtOAc/pentane = 1:19); ^{1}H NMR (400 MHz, $CDCl_3$) δ 2.90 (t, *J* = 7.6 Hz, 2H), 2.13 (t, *J* = 7.6 Hz, 2H), 2.07 – 2.00 (m, 3H), 1.72 – 1.67 (m, 2H); ^{13}C NMR (101 MHz, $CDCl_3$) δ 82.50, 69.56, 37.54, 31.84, 28.67, 13.32, -3.76. Spectra were consistent with previously reported data.[69]

(2-(3-(But-3-yn-1-yl)-3*H*-diazirin-3-yl)ethyl)triphenylphosphonium iodide (6)

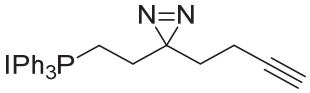

To a solution of iodide **15** (0.2621 g, 1.057 mmol) in dry acetonitrile (4.2 mL) in a microwave vial was added PPh_3 (1.386 g, 5.28 mmol) and the vial was sealed. The mixture was degassed and stirred at 70 °C overnight, concentrated under reduced pressure and purified by column chromatography (MeOH/DCM = 1:100 to 1:19) to afford the title compound as a white solid (0.539 g, 1.056 mmol, quant.). R_f = 0.49 (MeOH/DCM = 1:9); ^{1}H NMR (400 MHz, $CDCl_3$) δ 7.90 – 7.75 (m, 10H), 7.74 – 7.69 (m, 5H), 3.83 – 3.70 (m, 2H), 2.11 – 2.01 (m, 2H), 2.01 – 1.92 (m, 2H), 1.90 (t, *J* = 2.6 Hz, 1H), 1.85 – 1.72 (m, 2H); ^{13}C NMR (101 MHz, $CDCl_3$) δ 135.52 (d, *J* = 2.9 Hz), 133.85 (d, *J* = 10.1 Hz), 130.79 (d, *J* = 12.7 Hz), 117.42 (d, *J* = 86.6 Hz), 83.03, 69.60, 31.16, 28.42, 27.22 (d, *J* = 2.9 Hz), 18.71 (d, *J* = 51.8 Hz), 13.55; HRMS: Calculated for $[C_{25}H_{24}N_2P]^+$ 383.1672, found 383.1681.

(But-3-yn-1-yloxy)(*tert*-butyl)dimethylsilane (17)

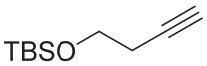

To a cooled (0 °C) solution of but-3-yn-1-ol (5.0 mL, 66 mmol) in dry DMF (150 mL) was added imidazole (6.75 g, 99 mmol) and subsequently TBSCl (11.95 g, 79 mmol) in portions. After 2 h, the reaction was quenched with H_2O (100 mL) and diluted with Et_2O (150 mL). The layers were separated and the aqueous layer extracted with Et_2O (150 mL). The combined organic layers were washed with brine (4 x 100 mL), dried over $MgSO_4$, filtered and concentrated under reduced pressure to afford the title compound as a clear liquid (11.95 g, 64.8 mmol, 98%). ^{1}H NMR (400 MHz, $CDCl_3$) δ 3.74 (t, *J* = 7.1 Hz, 2H), 2.40 (td, *J* = 7.1, 2.7 Hz, 2H), 1.96 (t, *J* = 2.7 Hz, 1H), 0.89 (s, 9H), 0.07 (s, 6H); ^{13}C NMR (101 MHz, $CDCl_3$) δ 81.66, 69.43, 61.87, 26.02, 22.98, -5.16. Spectra were consistent with previously reported data.[70]

5-((*Tert*-butyldimethylsilyl)oxy)pent-2-yn-1-ol (18)

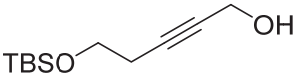

To a cooled (-40 °C) solution of alkyne **17** (26.76 g, 145 mmol) in dry THF (300 mL) under argon was added *n*-BuLi (61.0 mL, 152 mmol) dropwise over 10 min. After addition, it was stirred at -40 °C for 15 min and subsequently transferred through cannula to a flask containing a cooled (-40 °C) suspension of paraformaldehyde (13.08 g, 435 mmol) in dry THF (150 mL). After addition, the cooling bath was removed and the mixture was stirred for 1 h. It was then diluted with Et_2O (500 mL) and quenched by addition of brine (50 mL). The mixture was then washed with brine (150 mL) after which the organic layer was collected, dried over $MgSO_4$, filtered and concentrated under reduced pressure. The residue was purified through column chromatography (EtOAc/pentane = 1:19 to 1:4) to afford the title compound as a clear oil (25.46 g, 119 mmol, 82%). R_f = 0.22 (EtOAc/pentane = 1:9); ^{1}H NMR (400 MHz, $CDCl_3$) δ 4.23 (t, *J* = 2.2 Hz, 2H), 3.71 (t, *J* = 7.2 Hz, 2H), 2.42 (tt, *J* = 7.2, 2.1 Hz, 2H), 1.95 (bs, 1H), 0.89 (s, 9H), 0.06 (s, 6H); ^{13}C NMR (101 MHz, $CDCl_3$) δ 83.43, 79.63, 61.95, 51.39, 26.00, 23.23, 18.47, -5.16. Spectra were consistent with previously reported data.[71]

5-((*Tert*-butyldimethylsilyl)oxy)pent-2-yn-1-yl 4-methylbenzenesulfonate (19)

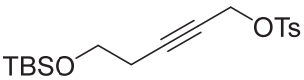

To a cooled (0 °C) solution of alcohol **18** (8.220 g, 38.3 mmol) in Et_2O (80 mL) was added TsCl (8.77 g, 46.0 mmol) followed by freshly pestled KOH (10.76 g, 192 mmol) in 10 portions over 5 min. The reaction was removed from the ice bath and after 45 min it was diluted with Et_2O (120 mL), cooled to 0 °C and poured into ice water (200 mL). The layers were separated and the aq. layer extracted with Et_2O (200 mL). The combined organic layers were washed with brine, dried over $MgSO_4$, filtered and concentrated under reduced pressure to afford the crude product (12.9622 g) as a slightly orange oil which was used without further purification due to its instability. R_f = 0.69 (EtOAc/pentane = 1:9); For NMR characterization an analytical sample was purified by column chromatography (EtOAc/pentane = 1:24); ^{1}H NMR (400 MHz, $CDCl_3$) δ 7.80 (d, *J* = 8.4 Hz, 2H), 7.34 (d, *J* = 8.0 Hz, 2H), 4.67 (t, *J* = 2.2 Hz, 2H), 3.59 (t, *J* = 7.1 Hz, 2H), 2.44 (s, 3H), 2.29 (tt, *J* = 7.1, 2.2 Hz, 2H), 0.87 (s, 9H), 0.03 (s, 6H); ^{13}C NMR (101 MHz, $CDCl_3$) δ 145.04, 133.37, 129.86, 128.24, 87.58, 73.03, 61.36, 58.66, 25.94, 23.17, 21.78, 18.40, -5.21. Spectra were consistent with previously reported data.[72]

9-((*Tert*-butyldimethylsilyl)oxy)nona-3,6-diyn-1-ol (20)

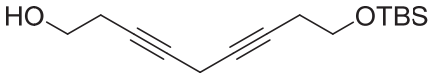

In a roundbottom flask, CuI (7.62 g, 40.0 mmol), NaI (6.00 g, 40.0 mmol) and Cs_2CO_3 (13.04 g, 40.0 mmol) were dried under vacuum at 90 °C for 2 h. The flask was backfilled with nitrogen and allowed to reach rt. Dry degassed DMF (70 mL) was added and the mixture was stirred for 10 min. But-3-yn-1-ol (3.22 mL, 42.6 mmol) was added to the mixture which was then stirred for 10 min. Sulfonate ester **19** (13.08 g, 35.5 mmol) was then added dropwise and the reaction was stirred overnight in the dark. The reaction was quenched with sat. aq. NH_4Cl (15 mL) and diluted with Et_2O (150 mL). After 20 min of stirring, the mixture was filtered over pad of celite and sand. The pad was rinsed with Et_2O (800 mL) and the resulting solution was washed with sat. aq. NH_4Cl (200 mL) and water (200 mL). The combined aq. layers were extracted with Et_2O (200 mL) and the combined organic layers were washed with brine (400 mL), dried over $MgSO_4$, filtered and concentrated under reduced pressure. Column chromatography (Et_2O/pentane = 1:10 to 1:4) afforded the title compound as a yellow oil (8.170 g, 30.7 mmol, 86%). R_f = 0.36 (EtOAc/pentane = 1:4); ^{1}H NMR (400 MHz, $CDCl_3$) δ 3.72 – 3.66 (m, 4H), 3.12 (p, *J* = 2.4 Hz, 2H), 2.43 (tt, *J* = 6.2, 2.4 Hz, 2H), 2.37 (tt, *J* = 7.2, 2.4 Hz, 2H), 0.88 (s, 9H), 0.06 (s, 6H); ^{13}C NMR (101 MHz, $CDCl_3$) δ 77.80, 77.07, 76.74, 75.37, 62.08, 61.22, 26.02, 23.24, 23.22, 18.49, 9.89, -5.13; HRMS: Calculated for $[C_{15}H_{26}O_2Si+H]^+$ 267.1775, found 267.1775.

(3*Z*,6*Z*)-9-((*Tert*-butyldimethylsilyl)oxy)nona-3,6-dien-1-ol (9)

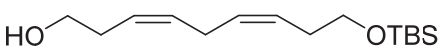

In a Schlenk flask, nickel acetate hydrate (0.300 g, 1.206 mmol) was added to 96% EtOH (15.08 mL) and purged with nitrogen. In a vial, $NaBH_4$ (0.046 g, 1.206 mmol) was added to a mixture of 96% EtOH (0.2 mL) and aq. NaOH (2 M, 11 µL) and the mixture was added dropwise to the Schlenk flask. The flask was

purged with H_2 and stirred for 20 min. Then, freshly distilled ethylenediamine (0.244 mL, 3.62 mmol) and alcohol **20** (1.6071 g, 6.03 mmol) were added and the reaction was stirred under H_2 atmosphere. After 2 h, additional catalyst was prepared in a Schlenk flask in 96% EtOH (5 mL) and added to the reaction via cannula. After 20 min of stirring the reaction was purged with N_2, the mixture was diluted with Et_2O (80 mL) and water (80 mL) and filtered over celite. The layers were separated, the organic layer was washed with water (80 mL) and the combined aq. layers were extracted with Et_2O (100 mL). The combined organic layers were washed with water (100 mL) and brine (100 mL), dried over $MgSO_4$, filtered and concentrated under reduced pressure. Column chromatography (EtOAc/pentane = 1:14.5 to 1:10.5) afforded the title compound (1.0363 g, 3.83 mmol, 64%) as a yellow oil. R_f = 0.69 (EtOAc/pentane = 1:2); ^{1}H NMR (400 MHz, $CDCl_3$) δ 5.58 – 5.49 (m, 1H), 5.47 – 5.35 (m, 3H), 3.65 (t, *J* = 6.5 Hz, 2H), 3.62 (t, *J* = 6.9 Hz, 2H), 2.84 (t, *J* = 5.7 Hz, 2H), 2.41 – 2.26 (m, 4H), 0.89 (s, 9H), 0.05 (s, 6H); ^{13}C NMR (101 MHz, $CDCl_3$) δ 131.42, 129.52, 126.55, 125.67, 62.98, 62.35, 31.25, 30.97, 26.10, 26.02, -5.12; HRMS: Calculated for $[C_{15}H_{30}O_2Si+H]^+$ 271.2088, found 271.2090.

Methyl pent-4-ynoate (22)

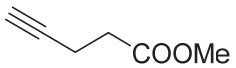

To a cooled (0 °C) solution of pent-4-ynoic acid (5.14 g, 52.4 mmol) in dry MeOH (200 mL) was added $SOCl_2$ (4.21 mL, 57.6 mmol) dropwise after which the reaction was allowed to reach rt overnight. The reaction was diluted with DCM (250 mL) and sat. aq. $NaHCO_3$ (500 mL). The layers were separated and the aq. layer extracted with DCM (200 mL). The combined organic layers were washed with brine (200 mL), dried over $MgSO_4$, filtered, concentrated under reduced pressure and coevaporated with DCM to afford the title compound as a clear oil (5.39 g, 48.1 mmol, 92%). R_f = 0.47 (EtOAc/pentane 1:19); ^{1}H NMR (400 MHz, $CDCl_3$) δ 3.71 (s, 3H), 2.60 – 2.54 (m, 2H), 2.54 – 2.48 (m, 2H), 1.99 (t, *J* = 2.5 Hz, 1H); ^{13}C NMR (101 MHz, $CDCl_3$) δ 172.31, 82.55, 69.12, 51.92, 33.23, 14.44. Spectra were consistent with previously reported data.[73]

Methyl 10-((*tert*-butyldimethylsilyl)oxy)deca-4,7-diynoate (23)

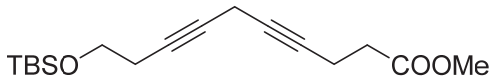

In a roundbottom flask, CuI (7.29 g, 38.3 mmol), NaI (5.74 g, 38.3 mmol) and Cs_2CO_3 (12.48 g, 38.3 mmol) were dried under vacuum for 6 h at 95 °C. The flask was refilled with nitrogen and allowed to cool to rt. Under stirring, dry degassed DMF (70 mL) was added and the mixture was stirred for 10 min. Then, alkyne **22** (5.389 g, 48.1 mmol) was added in one portion after which sulfonate ester **19** (12.97 g, 35.2 mmol) was added dropwise over 15 min and the reaction was stirred overnight. The reaction was diluted with Et_2O (320 mL) and quenched with sat. aq. NH_4Cl (12 mL) and stirred for 15 min. The mixture was filtered over celite and the filter was rinsed with Et_2O (1.5 L). The mixture was washed with sat. aq. NH_4Cl (100 mL) and water (100 mL), the combined aq. layers were extracted with Et_2O (100 mL) and the combined organic layers were washed with brine (5 x 100 mL). The organic layer was dried over $MgSO_4$, filtered and concentrated under reduced pressure. The residue was purified using neutralized silica (flushed with 0.5% Et_3N in pentane, EtOAc/pentane = 1:99 to 1:24) to afford the title compound as a clear oil (8.050 g, 26.1 mmol, 74%). R_f = 0.54 (EtOAc/pentane = 1:9); ^{1}H NMR (400 MHz, $CDCl_3$) δ 3.73 – 3.65 (m, 5H), 3.09 (t, *J* = 2.3 Hz, 2H), 2.55 – 2.46 (m, 4H), 2.40 – 2.33 (m, 2H), 0.88 (s, 9H), 0.06 (s, 6H); ^{13}C NMR (101 MHz, $CDCl_3$) δ 172.57, 78.55, 77.63, 75.45, 75.27, 62.09, 51.87, 33.49, 26.01, 23.22, 18.47, 14.76, 9.83, -5.15; HRMS: Calculated for $[C_{17}H_{28}O_3Si+H]^+$ 309.1881, found 309.1882.

Methyl (4*Z*,7*Z*)-10-((*tert*-butyldimethylsilyl)oxy)deca-4,7-dienoate (24)

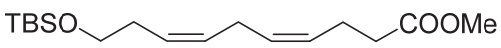

In a microwave vial, nickel acetate hydrate (0.169 g, 0.681 mmol) was dissolved in MeOH (2 mL) and purged with three vacuum/H_2 cycles. Under vigorous stirring, $NaBH_4$ (0.026 g, 0.681 mmol) was added in dry MeOH (1 mL). After 15 min, freshly distilled ethylenediamine (0.184 mL, 2.72 mmol) was added and the mixture was purged with a cycle of vacuum/H_2. After 15 min a solution of methyl ester **23** in MeOH (1 mL) was added and the mixture was purged with a cycle of vacuum/H_2. After 3 h, the mixture was purged with three vacuum/N_2 cycles, filtered over celite and concentrated under reduced pressure. The

residue was redissolved in Et_2O (10 mL), washed with sat. aq. NH_4Cl (5 mL) and brine (5 mL), dried over Na_2SO_4, filtered and concentrated under reduced pressure to afford the title compound as a yellow oil (0.0634 g, 0.203 mmol, 89%). R_f = 0.62 (EtOAc/pentane = 1:24); ^{1}H NMR (400 MHz, $CDCl_3$) δ 5.45 – 5.30 (m, 4H), 3.67 (s, 3H), 3.61 (t, *J* = 6.9 Hz, 2H), 2.81 (t, *J* = 5.8 Hz, 2H), 2.42 – 2.33 (m, 4H), 2.33 – 2.24 (m, 2H), 0.89 (s, 9H), 0.05 (s, 6H); ^{13}C NMR (101 MHz, $CDCl_3$) δ 173.68, 129.63, 129.56, 127.87, 126.44, 62.98, 51.68, 34.15, 31.24, 26.09, 25.82, 22.92, 18.50, -5.13; HRMS: Calculated for $[C_{17}H_{32}O_3Si\text{-}TBS+2H]^+$ 199.1329, found 199.1328.

Methyl (4*Z*,7*Z*)-10-hydroxydeca-4,7-dienoate (25)

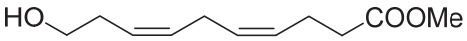

To a cooled (0 °C) solution of methyl ester **24** (0.7420 g, 2.374 mmol) in THF (25 mL) was added TBAF (1 M in THF, 3.56 mL, 3.56 mmol) and the mixture was allowed to reach rt. After 2 h, additional TBAF (1 M in THF, 0.475 mL, 0.475 mmol) was added. After 0.5 h the reaction was cooled to 0 °C, diluted with sat. aq. NH_4Cl (100 mL) and Et_2O (100 mL). The organic phase was collected and the aq. phase extracted with Et_2O (100 mL). The combined organic layers were washed with brine (2 x 100 mL), dried over $MgSO_4$, filtered and concentrated under reduced pressure. Column chromatography (EtOAc/pentane = 1:9 to 1:1) afforded the title compound as a clear oil (0.3361 g, 1.695 mmol, 71%). R_f = 0.52 (EtOAc/pentane = 1:1); ^{1}H NMR (500 MHz, $CDCl_3$) δ 5.59 – 5.49 (m, 1H), 5.48 – 5.33 (m, 3H), 3.70 – 3.62 (m, 5H), 2.90 – 2.80 (m, 2H), 2.46 – 2.33 (m, 6H), 1.69 (s, 1H); ^{13}C NMR (126 MHz, $CDCl_3$) δ 173.81, 130.99, 129.31, 128.07, 125.93, 62.31, 51.74, 34.08, 30.98, 25.84, 22.93; HRMS: Calculated for $[C_{11}H_{18}O_3+H]^+$ 199.1329, found 199.1329.

Methyl (4*Z*,7*Z*)-10-bromodeca-4,7-dienoate (26)

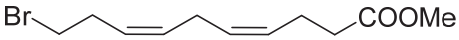

Alcohol **25** (0.4527 g, 2.283 mmol) was coevaporated three times with dry toluene, dissolved in dry DCM (10 mL) and cooled to -30 °C. CBr_4 (0.984 g, 2.97 mmol) was added and then PPh_3 (0.779 g, 2.97 mmol) was added in three portions over three min. After 30 min, the reaction was allowed to reach 0 °C and stirred for 1.5 h. The solvent was then removed under reduced pressure and the residue purified with column chromatography (Et_2O/pentane = 1:19 to 1:9) to afford the title compound as a clear oil (0.6031 g, 2.309 mmol, quant.). R_f = 0.71 (EtOAc/pentane = 1:19); ^{1}H NMR (400 MHz, $CDCl_3$) δ 5.57 – 5.47 (m, 1H), 5.47 – 5.32 (m, 3H), 3.68 (s, 3H), 3.38 (t, *J* = 7.1 Hz, 2H), 2.83 (t, *J* = 5.9 Hz, 2H), 2.65 (q, *J* = 7.1 Hz, 2H), 2.39 (m, 4H); ^{13}C NMR (101 MHz, $CDCl_3$) δ 173.58, 130.84, 128.94, 128.27, 126.53, 51.68, 34.03, 32.49, 30.86, 25.83, 22.90; HRMS: Calculated for $[C_{11}H_{17}BrO_2+H]^+$ 261.0485, found 261.0486.

((3*Z*,6*Z*)-10-Methoxy-10-oxodeca-3,6-dien-1-yl)triphenylphosphonium bromide (8)

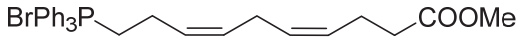

In a microwave vial, bromide **26** (0.2803 g, 1.073 mmol) and dry PPh_3 (0.422 g, 1.610 mmol) were dissolved in dry acetonitrile (7 mL) and the vial was sealed. The solvent was purged with three vacuum/N_2 cycles and the reaction was stirred at 92 °C for 5 days in the dark. The reaction was concentrated under a flow of N_2 and purified with column chromatography (MeOH/DCM = 1:99 to 1:5) to afford the title compound as a clear syrup (0.5751 g, 1.099 mmol, quant.). R_f = 0.19 (MeOH/DCM 1:9); ^{1}H NMR (500 MHz, $CDCl_3$) δ 7.92 – 7.77 (m, 10H), 7.75 – 7.72 (m, 5H), 5.69 – 5.56 (m, 1H), 5.42 – 5.32 (m, 1H), 5.32 – 5.22 (m, 2H), 3.91 – 3.81 (m, 2H), 3.63 (s, 3H), 2.58 (t, *J* = 7.0 Hz, 2H), 2.54 – 2.39 (m, 2H), 2.30 (td, *J* = 7.2, 1.2 Hz, 2H), 2.26 – 2.18 (m, 2H); ^{13}C NMR (126 MHz, $CDCl_3$) δ 173.41, 135.13 (d, *J* = 3.1 Hz), 133.68 (d, *J* = 10.1 Hz), 130.54 (d, *J* = 12.6 Hz), 130.17, 128.33 (d, *J* = 13.3 Hz), 126.54 (d, *J* = 14.7 Hz), 118.10 (d, *J* = 85.8 Hz) 51.53, 33.70, 25.49, 22.91 (d, *J* = 48.7 Hz), 22.69, 20.40 (d, *J* = 3.5 Hz). HRMS: Calculated for $[C_{29}H_{32}O_2P]^+$ 443.2134, found 443.2132.

Methyl (4*Z*,7*Z*,10*Z*,13*Z*,16*Z*)-19-((*tert*-butyldimethylsilyl)oxy)nonadeca-4,7,10,13,16-pentaenoate (29)

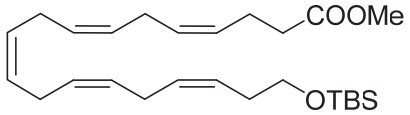

To a cooled (0 °C) solution of alcohol **9** (0.2784 g, 1.029 mmol) in dry DCM (4 mL) was added DMP (0.655 g, 1.544 mmol) and the reaction was allowed to reach rt. After 30 min, the mixture was

cooled to 0 °C, diluted with Et_2O (10 mL) and quenched with a mixture of sat. aq. $NaHCO_3$/10% (w/v) aq. $Na_2S_2O_3$ (1:1 (v/v), 10 mL) under vigorous stirring. The layers were separated and the organic layer washed with water (3 x 10 mL) and brine (10 mL), dried over Na_2SO_4, filtered and concentrated under reduced pressure at rt. The generated aldehyde **28** was used in the next reaction immediately.
Phosphonium salt **8** (0.9028 g, 1.725 mmol) was dried by coevaporation with dry toluene four times and dissolved in dry THF (9 mL) and dry HMPA (1.7 mL). It was cooled to -60 °C after which LiHMDS (1 M in THF, 1.65 mL, 1.65 mmol) was added dropwise. The reaction was stirred for 40 min at -60 °C and then cooled to -100 °C. A solution of aldehyde **28** in dry THF (2 mL) was added dropwise to the reaction. The reaction was stirred at -100 °C for 30 min and then allowed to reach 0 °C over 3 h. It was cooled to -20 °C and quenched with sat. aq. $NaHCO_3$ (10 mL). It was diluted with Et_2O (50 mL) and sat. aq. $NaHCO_3$ (20 mL), the aq. layer was isolated and extracted with Et_2O (30 mL) and the combined organic layers were washed with brine (3 x 20 mL), dried over Na_2SO_4, filtered and concentrated under reduced pressure. Column chromatography (Et_2O/pentane = 1:30 to 1:15) afforded the title compound as a clear oil (0.2529 g, 0.584 mmol, 57%). R_f = 0.57 (EtOAc/pentane = 1:20); ^{1}H NMR (400 MHz, $CDCl_3$) δ 5.50 – 5.29 (m, 10H), 3.67 (s, 3H), 3.62 (t, *J* = 7.0 Hz, 2H), 2.84 (dd, *J* = 7.0, 3.2 Hz, 8H), 2.38 (q, *J* = 3.1, 2.6 Hz, 4H), 2.30 (q, *J* = 6.9 Hz, 2H), 0.89 (s, 9H), 0.05 (s, 6H); ^{13}C NMR (101 MHz, $CDCl_3$) δ 129.68, 129.46, 128.49, 128.38, 128.36, 128.25, 128.20, 128.18, 128.01, 126.36, 63.00, 51.70, 34.15, 31.26, 26.10, 25.90, 25.77, 25.71, 22.93, 18.51, -5.12; HRMS: Calculated for $[C_{26}H_{44}O_3Si+H]^+$ 433.3133, found 433.3132.

Methyl (4*Z*,7*Z*,10*Z*,13*Z*,16*Z*)-19-hydroxynonadeca-4,7,10,13,16-pentaenoate (7)

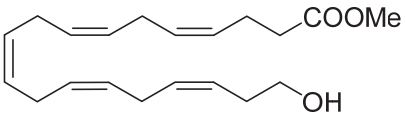

To a cooled (0 °C) solution of methyl ester **29** (0.5385 g, 1.244 mmol) in THF (12 mL) was added TBAF (1 M in THF, 1.87 mL, 1.87 mmol) and the reaction was allowed to reach rt. After 2 h, the reaction was quenched with sat. aq. NH_4Cl (100 mL) and diluted with Et_2O (100 mL). The layers were separated and the aq. layer was extracted with Et_2O (2 x 50 mL). The combined organic layers were washed with brine (100 mL), dried over $MgSO_4$, filtered and concentrated under reduced pressure. The residue was purified with column chromatography (EtOAc/pentane = 1:9 to 1:4) to afford the title compound (0.3453 g, 1.084 mmol, 87%) as a clear oil which was further purified with preparative HPLC (Gemini, 63 to 66% B in A over 12 min, 5 mL/min). R_f = 0.70 (EtOAc/pentane = 1:1); ^{1}H NMR (500 MHz, $CDCl_3$) δ 5.59 – 5.50 (m, 1H), 5.47 – 5.32 (m, 9H), 3.72 – 3.61 (m, 5H), 2.92 – 2.79 (m, 8H), 2.44 – 2.32 (m, 6H), 1.72 (bs, 1H); ^{13}C NMR (126 MHz, $CDCl_3$) δ 173.77, 131.17, 129.46, 128.41, 128.36, 128.31, 128.26, 128.21, 128.15, 128.00, 125.82, 62.34, 51.73, 34.13, 30.97, 25.90, 25.79, 25.78, 25.71, 22.92; HRMS: Calculated for $[C_{20}H_{30}O_3+H]^+$ 319.2268, found 319.2269.

Methyl (4*Z*,7*Z*,10*Z*,13*Z*,16*Z*,19*Z*)-21-(3-(but-3-yn-1-yl)-3*H*-diazirin-3-yl)henicosa-4,7,10,13,16,19-hexaenoate (31)

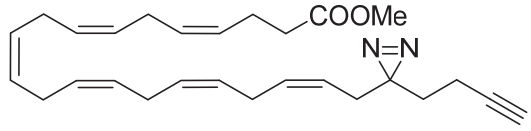

Alcohol **7** (0.0613 g, 0.192 mmol) was dissolved in dry DCM (2 mL), cooled to 0 °C and DMP (0.122 g, 0.289 mmol) was added. It was allowed to reach rt and stirred for 1 h, after which it was cooled to 0 °C, diluted with Et_2O (5 mL) and quenched by addition of a mixture of sat. aq. $NaHCO_3$/10% (w/v) aq. $Na_2S_2O_3$ (1:1 (v/v), 4 mL). It was stirred at rt until two layers appeared, after which the layers were separated, the aq. layer was extracted with Et_2O (10 mL) and the combined organic layers washed with brine (2 x 5 mL), dried over Na_2SO_4, filtered and concentrated under reduced pressure at rt. The formed aldehyde was dried by coevaporation with toluene at room temperature and used immediately. Phosphonium salt **6** (0.128 g, 0.250 mmol) was dried by coevaporation with toluene three times. It was suspended in dry THF (3 mL) and cooled to -70 °C after which KO*t*Bu (1.0 M in THF, 0.202 mL, 0.202 mmol) was added dropwise and the reaction was allowed to reach -50 °C over 1 h, then cooled to -105 °C. The aldehyde was dissolved in dry THF (2 mL) and added to the reaction via cannula dropwise. The reaction was allowed to reach -30 °C after which it was cooled to -80 °C. The reaction was diluted with dry Et_2O (5

mL) and quenched with sat. aq. $NaHCO_3$ (2 mL) under vigorous stirring. The reaction was further diluted with Et_2O (25 mL) and sat. aq. $NaHCO_3$ (25 mL), the layers were separated and the aq. layer extracted with Et_2O (25 mL). The combined organic layers were washed with brine (50 mL), dried over $MgSO_4$, filtered and concentrated under reduced pressure. Column chromatography of the residue (Et_2O/pentane = 1:49 to 1:19) afforded the title compound as a yellow oil (0.0306 g, 0.073 mmol, 38%). R_f = 0.68 (EtOAc/pentane = 1:9); ^{1}H NMR (500 MHz, $CDCl_3$) δ 5.53 (dtt, *J* = 10.4, 2.0, 7.2, 1H), 5.45 – 5.30 (m, 10H), 5.24 (dtt, *J* = 10.4, 1.6, 7.6 Hz, 1H), 3.67 (s, 3H), 2.89 – 2.79 (m, 8H), 2.75 (t, *J* = 7.3 Hz, 2H), 2.43 – 2.35 (m, 4H), 2.17 (d, *J* = 7.6 Hz, 2H), 2.04 – 1.98 (m, 3H), 1.65 (t, *J* = 7.4 Hz, 2H); ^{13}C NMR (126 MHz, $CDCl_3$) δ 173.66, 132.03, 129.43, 128.73, 128.42, 128.33, 128.25, 128.13, 128.03, 127.53, 121.94, 82.88, 69.26, 51.70, 34.13, 32.10, 31.27, 28.27, 25.86, 25.78, 25.71, 22.92, 13.45; HRMS: Calculated for $[C_{27}H_{36}N_2O_2+H]^+$ 421.2850, found 421.2849.

(4*Z*,7*Z*,10*Z*,13*Z*,16*Z*,19*Z*)-21-(3-(But-3-yn-1-yl)-3*H*-diazirin-3-yl)henicosa-4,7,10,13,16,19-hexaenoic acid (pac-DHA, 4)

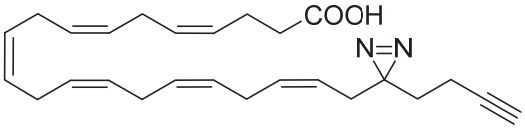

To a cooled (0 °C) solution of methyl ester **31** (0.0198 g, 0.047 mmol) in THF (2 mL) was added 1 M aq. LiOH (2 mL) and the reaction was allowed to reach rt overnight. It was then cooled to 0 °C, diluted with Et_2O (5 mL) and acidified with 1 M aq. HCl to pH <2. NaCl was added until saturation and the organic layer was isolated. The aq. layer was extracted with Et_2O (2 x 20 mL) and the combined organic layers were washed with brine (20 mL), dried over Na_2SO_4, filtered and concentrated under reduced pressure. Column chromatography of the residue (MeOH/DCM = 1:128 to 1:80) afforded the title compound as a slightly yellow oil (0.0159 g, 0.039 mmol, 83%). R_f = 0.47 (MeOH/DCM = 1:11); ^{1}H NMR (400 MHz, $CDCl_3$) δ 5.58 – 5.47 (m, 1H), 5.49 – 5.29 (m, 10H), 5.25 (dtt, *J* = 10.9, 7.6, 1.7 Hz, 1H), 2.84 (q, *J* = 6.9, 6.1 Hz, 8H), 2.75 (t, *J* = 7.0 Hz, 2H), 2.49 – 2.37 (m, 4H), 2.17 (dd, *J* = 7.6, 1.5 Hz, 2H), 2.05 – 1.96 (m, 3H), 1.65 (t, *J* = 7.3 Hz, 2H); ^{13}C NMR (101 MHz, $CDCl_3$) δ 178.86, 132.06, 129.72, 128.75, 128.44, 128.42, 128.32, 128.29, 128.16, 127.70, 127.55, 121.96, 82.91, 69.29, 33.99, 32.11, 31.29, 28.31, 25.88, 25.80, 25.74, 22.63, 13.48; HRMS: Calculated for $[C_{26}H_{34}N_2O_2+H]^+$ 407.2693, found 407.2693.

(4*Z*,7*Z*,10*Z*,13*Z*,15*E*,19*Z*)-21-(3-(But-3-yn-1-yl)-3*H*-diazirin-3-yl)-17-hydroxyhenicosa-4,7,10,13,15,19-hexaenoic acid (pac-17-HDHA, 5)

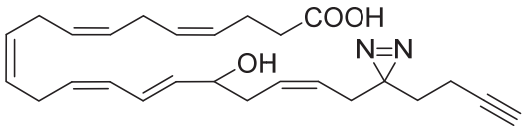

Carboxylic acid **4** (pac-DHA, 21 mg, 0.052 mmol) was dissolved in EtOH (5 mL) and added to a cooled (0 °C) borate buffer (50 mM boric acid in MilliQ, adjusted to pH 12 with NaOH, 500 mL). A solution of soy bean lipoxydase (SBLOX, L7395, Sigma, 50 mg) in borate buffer was added under vigorous stirring and air bubbling, and the reaction was stirred for 20 min. Then, aq. $NaBH_4$ (10.33 mmol, 10.33 mL) was added and the reaction was stirred for 15 min. Then, acetic acid (2.63 mL, 45.9 mmol) was added dropwise and after 15 min the reaction was extracted with $CHCl_3$ (4 x 200 mL). The combined organic layers were dried over Na_2SO_4, filtered, concentrated under reduced pressure and purified with column chromatography (MeOH/DCM = 1:99) and preparative HPLC (Nucleodur, 66 to 72% B in A over 12 min, 5 mL/min) to afford the title compound as a clear oil (1.0 mg, 2.37 µmol, 4.6%). Aliquots were taken to analyze purity by LC-MS and NMR and regioselectivity was confirmed by the *m/z* 285 fragment ion after hydrogenation and LC-MS. ^{1}H NMR (500 MHz, $CDCl_3$) δ 6.57 (dd, J = 15.1, 11.0 Hz, 1H), 5.98 (t, J = 10.9 Hz, 1H), 5.64 (dd, J = 15.2, 6.3 Hz, 1H), 5.58 – 5.32 (m, 9H), 4.16 – 4.09 (m, 1H), 2.97 (t, J = 7.0 Hz, 2H), 2.91 – 2.80 (m, 4H), 2.45 – 2.39 (m, 4H), 2.07 – 1.98 (m, 5H), 1.76 – 1.68 (m, 4H), 1.62 – 1.58 (m, 1H). HRMS: Calculated for $[C_{26}H_{34}N_2O_3+Na]^+$ 445.2462, found 445.2459.

Supplementary data

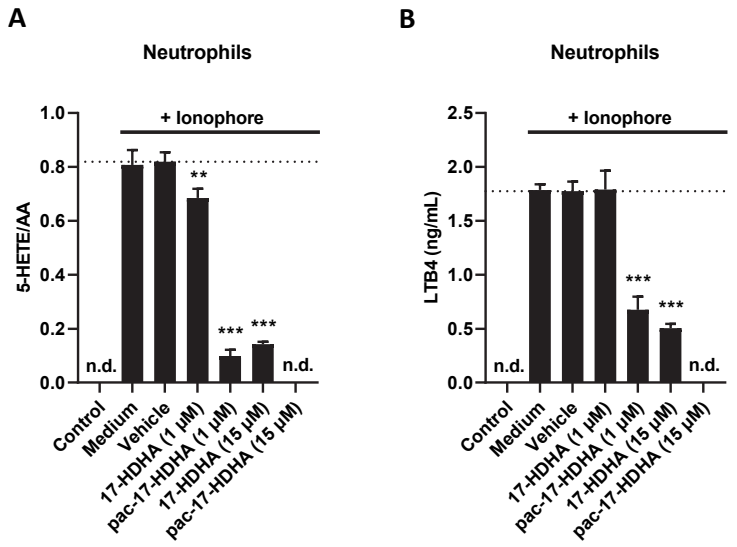

Figure S1 | Effect of 17-HDHA and pac-17-HDHA (5) on neutrophils. (A) 5-HETE/AA ratio and **(B)** LTB4 (LC-MS/MS) produced by ionophore-stimulated neutrophils. Data represent means ± SD of representative donor (n = 3). ** p <0.01; *** p <0.001 in comparison to ionophore-treated control (dotted line) using a one-way ANOVA with Dunnett's multiple comparisons correction. n.d.; not detected.

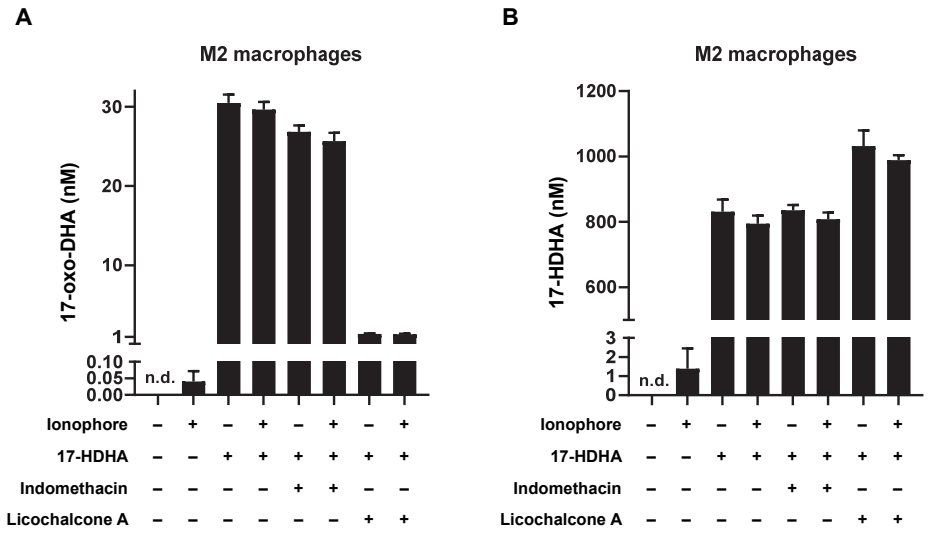

Figure S2 | Stimulation of M2 macrophages results in detectable formation of 17-HDHA and 17-oxo-DHA. (A) 17-oxo-DHA and **(B)** 17-HDHA measured in M2 macrophages shows that inhibition of PTGR1 by indomethacin and licochalcone A reduces conversion of 17-HDHA to 17-oxo-DHA. Cells were pretreated for 30 min with 10 µM indomethacin, licochalcone A or vehicle before treatment with 17-HDHA (15 µM) or vehicle for 2 h. Data represent means ± SD of representative donor (n = 2-3). One-way ANOVA between all conditions with Tukey's multiple comparisons correction: no significant difference between stimulated and unstimulated conditions.

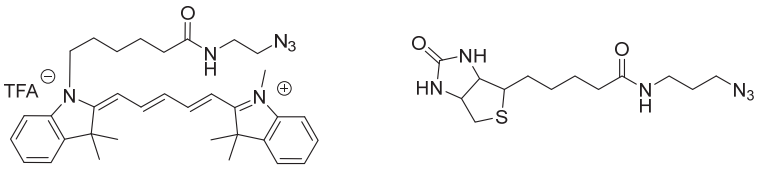

Cy5-N_3 (**32**) biotin-N_3 (**33**)

Figure S3 | Structures of Cy5-N_3 (32) and biotin-N_3 (33).

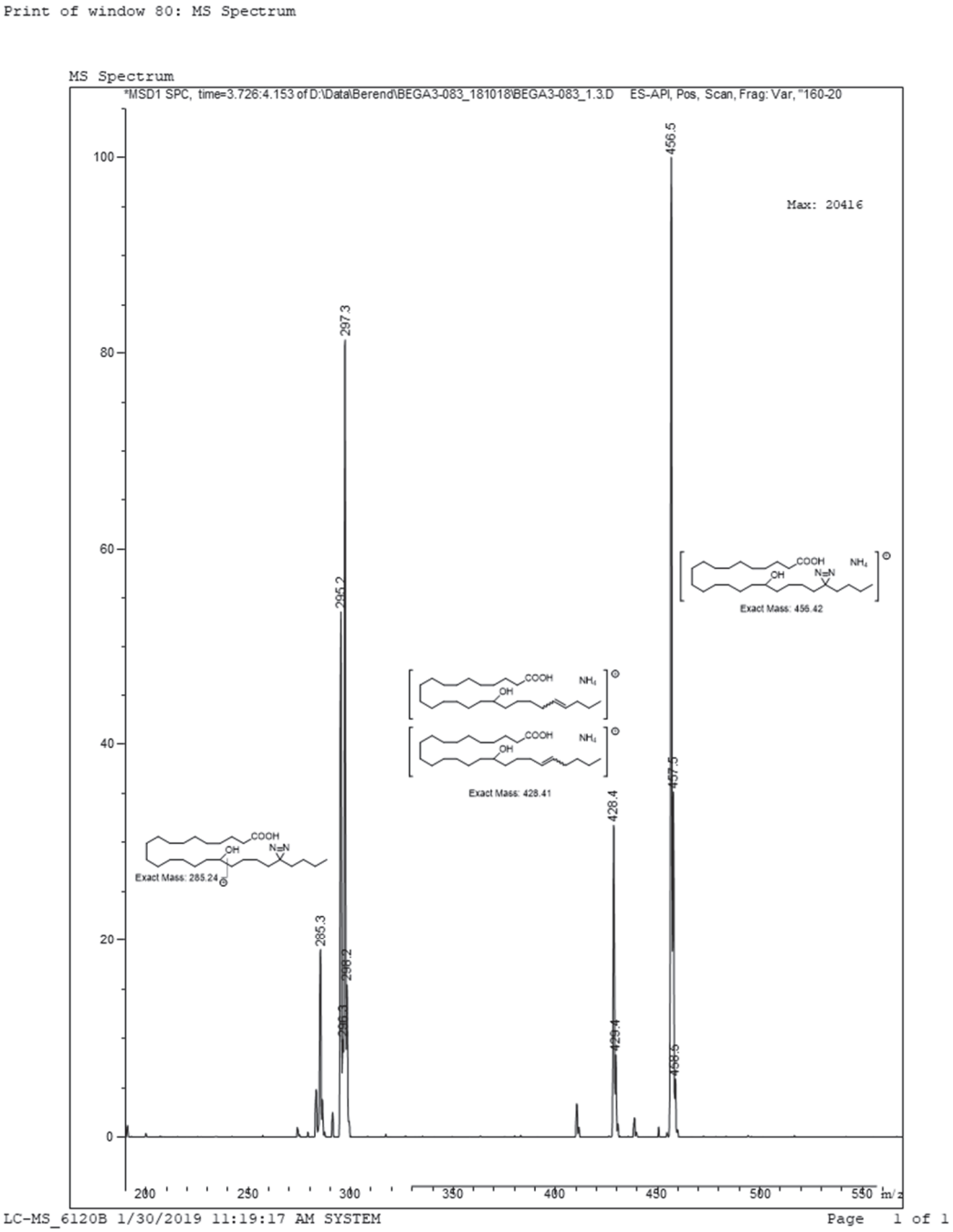

Figure S4 | Fragmentation pattern of hydrogenated pac-17-HDHA (5).

Table S2 | Proteins significantly UV-enriched by pac-17-HDHA (5) in M2 macrophages.

Gene name	Unique peptides	Description	UV/no UV pac-17-HDHA (5)	p-value	UV/ no UV pac-DHA (4)	Enrichment pac-17-HDHA/pac-DHA
DHRS4	10	Dehydrogenase/reductase SDR family member 4	56.45	0.0062	8.36	6.75
HSD3B7	3	3 beta-hydroxysteroid dehydrogenase type 7	51.86	0.0361	4.36	11.88
VDAC1	6	Voltage-dependent anion-selective channel protein 1	41.80	0.0025	27.96	1.50
ECH1	14	Delta(3,5)-Delta(2,4)-dienoyl-CoA isomerase	19.25	0.0062	18.43	1.04
ERAP1	20	Endoplasmic reticulum aminopeptidase 1	13.95	0.0109	1.28	10.94
PTGR1	**11**	**Prostaglandin reductase 1**	**11.28**	**0.0038**	**1.47**	**7.67**
APOL2	4	Apolipoprotein L2	9.97	0.0007	37.83	0.26
CERS2	2	Ceramide synthase 2	8.46	0.0022	6.30	1.34
SCP2	3	Non-specific lipid-transfer protein	7.60	0.0006	5.91	1.29
PLIN2	11	Perilipin-2	6.62	0.0052	24.32	0.27
PLIN3	2	Perilipin-3	6.22	0.0470	24.45	0.25
DECR1	4	2,4-dienoyl-CoA reductase, mitochondrial	6.19	0.0017	1.66	3.72
TMEM33	4	Transmembrane protein 33	4.95	0.0022	6.98	0.71
RAB1C	2	Putative Ras-related protein Rab-1C	4.75	0.0252	15.33	0.31
AGPS	2	Alkyldihydroxyacetonephosphate synthase peroxisomal	4.70	0.0087	2.90	1.62
DHRS1	5	Dehydrogenase/reductase SDR family member 1	4.64	0.0037	2.50	1.85
SRPRB	5	Signal recognition particle receptor subunit beta	4.04	0.0231	5.66	0.71
VDAC2	7	Voltage-dependent anion-selective channel protein 2	3.99	0.0062	16.94	0.24
METTL7A	2	Methyltransferase-like protein 7A	3.98	0.0067	23.57	0.17
SNX5	2	Sorting nexin-5	3.90	0.0115	2.12	1.84
FABP5	2	Fatty acid-binding protein epidermal	3.72	0.0328	1.00	3.72
IFI30	3	Gamma-interferon-inducible lysosomal thiol reductase	3.56	0.0057	5.16	0.69
HSD17B4	28	Peroxisomal multifunctional enzyme type 2	3.23	0.0073	2.47	1.31
SCAMP2	2	Secretory carrier-associated membrane protein 2	2.85	0.0065	12.45	0.23
HSD17B11	2	Estradiol 17-beta-dehydrogenase 11	2.65	0.0426	14.22	0.19
IDH1	8	Isocitrate dehydrogenase [NADP] cytoplasmic	2.65	0.0195	0.87	3.03
BCAP31	3	B-cell receptor-associated protein 31	2.64	0.0287	2.07	1.28
SQOR	6	Sulfide:quinone oxidoreductase, mitochondrial	2.61	0.0036	0.95	2.75
NCEH1	6	Neutral cholesterol ester hydrolase 1	2.59	0.0191	2.32	1.12
TBXAS1	5	Thromboxane-A synthase	2.33	0.0099	2.61	0.89
EPHX1	6	Epoxide hydrolase 1	2.26	0.0022	1.36	1.66
ALDH1A1	17	Retinal dehydrogenase 1	2.24	0.0037	0.84	2.68
ALDH2	16	Aldehyde dehydrogenase mitochondrial	2.03	0.0040	0.78	2.61

References

(1) Calder, P. C. Omega-3 Fatty Acids and Inflammatory Processes: From Molecules to Man. *Biochem. Soc. Trans.* **2017**, *45* (5), 1105–1115.

(2) Layé, S.; Nadjar, A.; Joffre, C.; Bazinet, R. P. Anti-Inflammatory Effects of Omega-3 Fatty Acids in the Brain: Physiological Mechanisms and Relevance to Pharmacology. *Pharmacol. Rev.* **2018**, *70* (1), 12–38.

(3) Larrieu, T.; Layé, S. Food for Mood: Relevance of Nutritional Omega-3 Fatty Acids for Depression and Anxiety. *Front. Physiol.* **2018**, *9*, 1047.

(4) Calder, P. C. Marine Omega-3 Fatty Acids and Inflammatory Processes: Effects, Mechanisms and Clinical Relevance. *Biochim. Biophys. Acta BBA - Mol. Cell Biol. Lipids* **2015**, *1851* (4), 469–484.

(5) Proudman, S. M.; James, M. J.; Spargo, L. D.; Metcalf, R. G.; Sullivan, T. R.; Rischmueller, M.; Flabouris, K.; Wechalekar, M. D.; Lee, A. T.; Cleland, L. G. Fish Oil in Recent Onset Rheumatoid Arthritis: A Randomised, Double-Blind Controlled Trial within Algorithm-Based Drug Use. *Ann. Rheum. Dis.* **2015**, *74* (1), 89–95.

(6) Gioxari, A.; Kaliora, A. C.; Marantidou, F.; Panagiotakos, D. P. Intake of ω-3 Polyunsaturated Fatty Acids in Patients with Rheumatoid Arthritis: A Systematic Review and Meta-Analysis. *Nutrition* **2018**, *45*, 114-124.e4.

(7) Navarini, L.; Afeltra, A.; Gallo Afflitto, G.; Margiotta, D. P. E. Polyunsaturated Fatty Acids: Any Role in Rheumatoid Arthritis? *Lipids Health Dis.* **2017**, *16* (1), 197.

(8) Serhan, C. N. Resolution Phase of Inflammation: Novel Endogenous Anti-Inflammatory and Proresolving Lipid Mediators and Pathways. *Annu. Rev. Immunol.* **2007**, *25* (1), 101–137.

(9) Serhan, C. N. Pro-Resolving Lipid Mediators Are Leads for Resolution Physiology. *Nature* **2014**, *510* (7503), 92–101.

(10) Barnig, C.; Bezema, T.; Calder, P. C.; Charloux, A.; Frossard, N.; Garssen, J.; Haworth, O.; Dilevskaya, K.; Levi-Schaffer, F.; Lonsdorfer, E.; Wauben, M.; Kraneveld, A. D.; te Velde, A. A. Activation of Resolution Pathways to Prevent and Fight Chronic Inflammation: Lessons From Asthma and Inflammatory Bowel Disease. *Front. Immunol.* **2019**, *10*, 1699.

(11) Schett, G.; Neurath, M. F. Resolution of Chronic Inflammatory Disease: Universal and Tissue-Specific Concepts. *Nat. Commun.* **2018**, *9* (1), 1–8.

(12) Tabas, I.; Glass, C. K. Anti-Inflammatory Therapy in Chronic Disease: Challenges and Opportunities. *Science* **2013**, *339* (6116), 166–172.

(13) Serhan, C. N.; Fredman, G.; Yang, R.; Karamnov, S.; Belayev, L. S.; Bazan, N. G.; Zhu, M.; Winkler, J. W.; Petasis, N. A. Novel Proresolving Aspirin-Triggered DHA Pathway. *Chem. Biol.* **2011**, *18* (8), 976–987.

(14) Weylandt, K. H.; Chiu, C.-Y.; Gomolka, B.; Waechter, S. F.; Wiedenmann, B. Omega-3 Fatty Acids and Their Lipid Mediators: Towards an Understanding of Resolvin and Protectin Formation. *Prostaglandins Other Lipid Mediat.* **2012**, *97* (3–4), 73–82.

(15) Valdes, A. M.; Ravipati, S.; Menni, C.; Abhishek, A.; Metrustry, S.; Harris, J.; Nessa, A.; Williams, F. M. K.; Spector, T. D.; Doherty, M.; Chapman, V.; Barrett, D. A. Association of the Resolvin Precursor 17-HDHA, but Not D- or E- Series Resolvins, with Heat Pain Sensitivity and Osteoarthritis Pain in Humans. *Sci. Rep.* **2017**, *7* (1), 10748.

(16) Bento, A. F.; Claudino, R. F.; Dutra, R. C.; Marcon, R.; Calixto, J. B. Omega-3 Fatty Acid-Derived Mediators 17(R)-Hydroxy Docosahexaenoic Acid, Aspirin-Triggered Resolvin D1 and Resolvin D2 Prevent Experimental Colitis in Mice. *J. Immunol.* **2011**, *187* (4), 1957–1969.

(17) Duffield, J. S.; Hong, S.; Vaidya, V. S.; Lu, Y.; Fredman, G.; Serhan, C. N.; Bonventre, J. V. Resolvin D Series and Protectin D1 Mitigate Acute Kidney Injury. *J. Immunol.* **2006**, *177* (9), 5902–5911.

(18) Lima-Garcia, J. F.; Dutra, R. C.; Silva, K. da; Motta, E. M.; Campos, M. M.; Calixto, J. B. The Precursor of Resolvin D Series and Aspirin-Triggered Resolvin D1 Display Anti-Hyperalgesic Properties in Adjuvant-Induced Arthritis in Rats. *Br. J. Pharmacol.* **2011**, *164* (2), 278–293.

(19) González-Périz, A.; Planagumà, A.; Gronert, K.; Miquel, R.; López-Parra, M.; Titos, E.; Horrillo, R.; Ferré, N.; Deulofeu, R.; Arroyo, V.; Rodés, J.; Clària, J. Docosahexaenoic Acid (DHA) Blunts Liver Injury by Conversion to Protective Lipid Mediators: Protectin D1 and 17S-Hydroxy-DHA. *FASEB J.* **2006**, *20* (14), 2537–2539.

(20) von Hegedus, J. H.; Kahnt, A. S.; Ebert, R.; Heijink, M.; Toes, R. E. M.; Giera, M.; Ioan-Facsinay, A. Toll-like Receptor Signaling Induces a Temporal Switch towards a Resolving Lipid Profile in Monocyte-Derived Macrophages. *Biochim. Biophys. Acta BBA - Mol. Cell Biol. Lipids* **2020**, *1865* (9), 158740.

(21) Chiu, C.-Y.; Gomolka, B.; Dierkes, C.; Huang, N. R.; Schroeder, M.; Purschke, M.; Manstein, D.; Dangi, B.; Weylandt, K. H. Omega-6 Docosapentaenoic Acid-Derived Resolvins and 17-Hydroxydocosahexaenoic Acid Modulate Macrophage Function and Alleviate Experimental Colitis. *Inflamm. Res.* **2012**, *61* (9), 967–976.

(22) Dalli, J.; Winkler, J. W.; Colas, R. A.; Arnardottir, H.; Cheng, C.-Y. C.; Chiang, N.; Petasis, N. A.; Serhan, C. N. Resolvin D3 and Aspirin-Triggered Resolvin D3 Are Potent Immunoresolvents. *Chem. Biol.* **2013**, *20* (2), 188–201.

(23) Niphakis, M. J.; Lum, K. M.; Cognetta III, A. B.; Correia, B. E.; Ichu, T.-A.; Olucha, J.; Brown, S. J.; Kundu, S.; Piscitelli, F.; Rosen, H.; Cravatt, B. F. A Global Map of Lipid-Binding Proteins and Their Ligandability in Cells. *Cell* **2015**, *161* (7), 1668–1680.
(24) Hulce, J. J.; Cognetta, A. B.; Niphakis, M. J.; Tully, S. E.; Cravatt, B. F. Proteome-Wide Mapping of Cholesterol-Interacting Proteins in Mammalian Cells. *Nat. Methods* **2013**, *10* (3), 259–264.
(25) Rowland, M. M.; Bostic, H. E.; Gong, D.; Speers, A. E.; Lucas, N.; Cho, W.; Cravatt, B. F.; Best, M. D. Phosphatidylinositol 3,4,5-Trisphosphate Activity Probes for the Labeling and Proteomic Characterization of Protein Binding Partners. *Biochemistry* **2011**, *50* (51), 11143–11161.
(26) Wang, D.; Du, S.; Cazenave-Gassiot, A.; Ge, J.; Lee, J.-S.; Wenk, M. R.; Yao, S. Q. Global Mapping of Protein–Lipid Interactions by Using Modified Choline-Containing Phospholipids Metabolically Synthesized in Live Cells. *Angew. Chem.* **2017**, *129* (21), 5923–5927.
(27) Haberkant, P.; Raijmakers, R.; Wildwater, M.; Sachsenheimer, T.; Brügger, B.; Maeda, K.; Houweling, M.; Gavin, A.-C.; Schultz, C.; van Meer, G.; Heck, A. J. R.; Holthuis, J. C. M. In Vivo Profiling and Visualization of Cellular Protein–Lipid Interactions Using Bifunctional Fatty Acids. *Angew. Chem. Int. Ed.* **2013**, *52* (14), 4033–4038.
(28) Höglinger, D.; Nadler, A.; Haberkant, P.; Kirkpatrick, J.; Schifferer, M.; Stein, F.; Hauke, S.; Porter, F. D.; Schultz, C. Trifunctional Lipid Probes for Comprehensive Studies of Single Lipid Species in Living Cells. *Proc. Natl. Acad. Sci.* **2017**, *114* (7), 1566–1571.
(29) Haberkant, P.; Stein, F.; Höglinger, D.; Gerl, M. J.; Brügger, B.; Van Veldhoven, P. P.; Krijgsveld, J.; Gavin, A.-C.; Schultz, C. Bifunctional Sphingosine for Cell-Based Analysis of Protein-Sphingolipid Interactions. *ACS Chem. Biol.* **2016**, *11* (1), 222–230.
(30) Zhuang, S.; Li, Q.; Cai, L.; Wang, C.; Lei, X. Chemoproteomic Profiling of Bile Acid Interacting Proteins. *ACS Cent. Sci.* **2017**, *3* (5), 501–509.
(31) Macklin, T. K.; Micalizio, G. C. Convergent and Stereospecific Synthesis of Complex Skipped Polyenes and Polyunsaturated Fatty Acids. *Nat. Chem.* **2010**, *2* (8), 638–643.
(32) Lum, K. M.; Sato, Y.; Beyer, B. A.; Plaisted, W. C.; Anglin, J. L.; Lairson, L. L.; Cravatt, B. F. Mapping Protein Targets of Bioactive Small Molecules Using Lipid-Based Chemical Proteomics. *ACS Chem. Biol.* **2017**, *12* (10), 2671–2681.
(33) Koenders, S. T. A.; Gagestein, B.; van der Stelt, M. Opportunities for Lipid-Based Probes in the Field of Immunology. In *Activity-Based Protein Profiling*; Cravatt, B. F., Hsu, K.-L., Weerapana, E., Eds.; Current Topics in Microbiology and Immunology; Springer International Publishing: Cham, 2019; pp 283–319.
(34) Bockelmann, S.; Mina, J. G. M.; Korneev, S.; Hassan, D. G.; Müller, D.; Hilderink, A.; Vlieg, H. C.; Raijmakers, R.; Heck, A. J. R.; Haberkant, P.; Holthuis, J. C. M. A Search for Ceramide Binding Proteins Using Bifunctional Lipid Analogs Yields CERT-Related Protein StarD7. *J. Lipid Res.* **2018**, *59* (3), 515–530.
(35) Mbarik, M.; Biam, R. S.; Robichaud, P.-P.; Surette, M. E. The Impact of PUFA on Cell Responses: Caution Should Be Exercised When Selecting PUFA Concentrations in Cell Culture. *Prostaglandins Leukot. Essent. Fatty Acids* **2020**, 102083.
(36) Li, Z.; Hao, P.; Li, L.; Tan, C. Y. J.; Cheng, X.; Chen, G. Y. J.; Sze, S. K.; Shen, H.-M.; Yao, S. Q. Design and Synthesis of Minimalist Terminal Alkyne-Containing Diazirine Photo-Crosslinkers and Their Incorporation into Kinase Inhibitors for Cell- and Tissue-Based Proteome Profiling. *Angew. Chem.* **2013**, *125* (33), 8713–8718.
(37) Kleiner, P.; Heydenreuter, W.; Stahl, M.; Korotkov, V. S.; Sieber, S. A. A Whole Proteome Inventory of Background Photocrosslinker Binding. *Angew. Chem. Int. Ed.* **2017**, *56* (5), 1396–1401.
(38) Sakurai, K. Photoaffinity Probes for Identification of Carbohydrate-Binding Proteins. *Asian J. Org. Chem.* **2015**, *4* (2), 116–126.
(39) Vik, A.; Hansen, T. V. Synthetic Manipulations of Polyunsaturated Fatty Acids as a Convenient Strategy for the Synthesis of Bioactive Compounds. *Org. Biomol. Chem.* **2018**, *16* (48), 9319–9333.
(40) Balas, L.; Durand, T.; Saha, S.; Johnson, I.; Mukhopadhyay, S. Total Synthesis of Photoactivatable or Fluorescent Anandamide Probes: Novel Bioactive Compounds with Angiogenic Activity. *J. Med. Chem.* **2009**, *52* (4), 1005–1017.
(41) Heitz, M. P.; Wagner, A.; Mioskowski, C.; Noel, J. P.; Beaucourt, J. P. Synthesis of All-Cis-1-Bromo-4,7,10,13-Nonadecatetraene: A Precursor to C-1-Labeled Arachidonic Acid. *J. Org. Chem.* **1989**, *54* (2), 500–503.
(42) Saha, G.; Basu, M. K.; Kim, S.; Jung, Y.-J.; Adiyaman, Y.; Adiyaman, M.; Powell, W. S.; FitzGerald, G. A.; Rokach, J. A Convenient Strategy for the Synthesis of β,γ-Unsaturated Aldehydes and Acids. A Construction of Skipped Dienes. *Tetrahedron Lett.* **1999**, *40* (40), 7179–7183.
(43) Rosell, M.; Villa, M.; Durand, T.; Galano, J.-M.; Vercauteren, J.; Crauste, C. Total Syntheses of Two Bis-Allylic-Deuterated DHA Analogues. *Asian J. Org. Chem.* **2017**, *6* (3), 322–334.
(44) Coffa, G.; Imber, A. N.; Maguire, B. C.; Laxmikanthan, G.; Schneider, C.; Gaffney, B. J.; Brash, A. R. On the Relationships of Substrate Orientation, Hydrogen Abstraction, and Product Stereochemistry in Single and Double Dioxygenations by Soybean Lipoxygenase-1 and Its Ala542Gly Mutant. *J. Biol. Chem.* **2005**, *280* (46), 38756–38766.

(45) Chechetkin, I. R.; Osipova, E. V.; Tarasova, N. B.; Mukhitova, F. K.; Hamberg, M.; Gogolev, Y. V.; Grechkin, A. N. Specificity of Oxidation of Linoleic Acid Homologs by Plant Lipoxygenases. *Biochem. Mosc.* **2009**, *74* (8), 855–861.

(46) Dobson, E. P.; Barrow, C. J.; Kralovec, J. A.; Adcock, J. L. Controlled Formation of Mono- and Dihydroxy-Resolvins from EPA and DHA Using Soybean 15-Lipoxygenase. *J. Lipid Res.* **2013**, *54* (5), 1439–1447.

(47) Luo, Y.; Blex, C.; Baessler, O.; Glinski, M.; Dreger, M.; Sefkow, M.; Köster, H. The CAMP Capture Compound Mass Spectrometry as a Novel Tool for Targeting CAMP-Binding Proteins: FROM PROTEIN KINASE A TO POTASSIUM/SODIUM HYPERPOLARIZATION-ACTIVATED CYCLIC NUCLEOTIDE-GATED CHANNELS. *Mol. Cell. Proteomics* **2009**, *8* (12), 2843–2856.

(48) Himo, F.; Lovell, T.; Hilgraf, R.; Rostovtsev, V. V.; Noodleman, L.; Sharpless, K. B.; Fokin, V. V. Copper(I)-Catalyzed Synthesis of Azoles. DFT Study Predicts Unprecedented Reactivity and Intermediates. *J. Am. Chem. Soc.* **2005**, *127* (1), 210–216.

(49) Mellacheruvu, D.; Wright, Z.; Couzens, A. L.; Lambert, J. P.; St-Denis, N. A.; Li, T.; Miteva, Y. V.; Hauri, S.; Sardiu, M. E.; Low, T. Y.; Halim, V. A.; Bagshaw, R. D.; Hubner, N. C.; Al-Hakim, A.; Bouchard, A.; Faubert, D.; Fermin, D.; Dunham, W. H.; Goudreault, M.; Lin, Z. Y.; Badillo, B. G.; Pawson, T.; Durocher, D.; Coulombe, B.; Aebersold, R.; Superti-Furga, G.; Colinge, J.; Heck, A. J. R.; Choi, H.; Gstaiger, M.; Mohammed, S.; Cristea, I. M.; Bennett, K. L.; Washburn, M. P.; Raught, B.; Ewing, R. M.; Gingras, A. C.; Nesvizhskii, A. I. The CRAPome: A Contaminant Repository for Affinity Purification-Mass Spectrometry Data. *Nat. Methods* **2013**, *10* (8), 730–736.

(50) Huang, D. W.; Sherman, B. T.; Lempicki, R. A. Systematic and Integrative Analysis of Large Gene Lists Using DAVID Bioinformatics Resources. *Nat. Protoc.* **2009**, *4* (1), 44–57.

(51) Mesa, J.; Alsina, C.; Oppermann, U.; Parés, X.; Farrés, J.; Porté, S. Human Prostaglandin Reductase 1 (PGR1): Substrate Specificity, Inhibitor Analysis and Site-Directed Mutagenesis. *Chem. Biol. Interact.* **2015**, *234*, 105–113.

(52) Kang, G.-J.; Lee, H.-J.; Byun, H. J.; Kim, E. J.; Kim, H. J.; Park, M. K.; Lee, C.-H. Novel Involvement of MiR-522-3p in High-Mobility Group Box 1-Induced Prostaglandin Reductase 1 Expression and Reduction of Phagocytosis. *Biochim. Biophys. Acta BBA - Mol. Cell Res.* **2017**, *1864* (4), 625–633.

(53) Yamamoto, T.; Yokomizo, T.; Nakao, A.; Izumi, T.; Shimizu, T. Immunohistochemical Localization of Guinea-Pig Leukotriene B4 12-Hydroxydehydrogenase/15-Ketoprostaglandin 13-Reductase. *Eur. J. Biochem.* **2001**, *268* (23), 6105–6113.

(54) Yokomizo, T.; Izumi, T.; Takahashi, T.; Kasama, T.; Kobayashi, Y.; Sato, F.; Taketani, Y.; Shimizu, T. Enzymatic Inactivation of Leukotriene B4 by a Novel Enzyme Found in the Porcine Kidney. Purification and Properties of Leukotriene B4 12-Hydroxydehydrogenase. *J. Biol. Chem.* **1993**, *268* (24), 18128–18135.

(55) Hori, T.; Ishijima, J.; Yokomizo, T.; Ago, H.; Shimizu, T.; Miyano, M. Crystal Structure of Anti-Configuration of Indomethacin and Leukotriene B4 12-Hydroxydehydrogenase/15-Oxo-Prostaglandin 13-Reductase Complex Reveals the Structural Basis of Broad Spectrum Indomethacin Efficacy. *J. Biochem. (Tokyo)* **2006**, *140* (3), 457–466.

(56) Roberts, L. S.; Yan, P.; Bateman, L. A.; Nomura, D. K. Mapping Novel Metabolic Nodes Targeted by Anti-Cancer Drugs That Impair Triple-Negative Breast Cancer Pathogenicity. *ACS Chem. Biol.* **2017**, *12* (4), 1133–1140.

(57) Yue, W. W.; Shafqat, N.; Krojer, T.; Pike, A. C. W.; von Delft, F.; Sethi, R.; Savitsky, P.; Johansson, C.; Arrowsmith, C.; Weigelt, J.; Edwards, A.; Bountra, C.; Oppermann, U. Crystal Structure of Human Leukotriene B4 12-Hydroxydehydrogenase in Complex with Nadp and Raloxifene. No. RCS Protein Data Bank 2Y05.

(58) Groeger, A. L.; Cipollina, C.; Cole, M. P.; Woodcock, S. R.; Bonacci, G.; Rudolph, T. K.; Rudolph, V.; Freeman, B. A.; Schopfer, F. J. Cyclooxygenase-2 Generates Anti-Inflammatory Mediators from Omega-3 Fatty Acids. *Nat. Chem. Biol.* **2010**, *6* (6), 433–441.

(59) Cipollina, C.; Vincenzo, S. D.; Siena, L.; Sano, C. D.; Gjomarkaj, M.; Pace, E. 17-Oxo-DHA Displays Additive Anti-Inflammatory Effects with Fluticasone Propionate and Inhibits the NLRP3 Inflammasome. *Sci. Rep.* **2016**, *6* (1), 1–12.

(60) Egawa, D.; Itoh, T.; Akiyama, Y.; Saito, T.; Yamamoto, K. 17-OxoDHA Is a PPARα/γ Dual Covalent Modifier and Agonist. *ACS Chem. Biol.* **2016**, *11* (9), 2447–2455.

(61) Jamil, M. U.; Kim, J.; Yum, H.-W.; Kim, S. H.; Kim, S.-J.; Kim, D.-H.; Cho, N.-C.; Na, H.-K.; Surh, Y.-J. 17-Oxo-Docosahexaenoic Acid Induces Nrf2-Mediated Expression of Heme Oxygenase-1 in Mouse Skin in Vivo and in Cultured Murine Epidermal Cells. *Arch. Biochem. Biophys.* **2020**, *679*, 108156.

(62) Cipollina, C.; Di Vincenzo, S.; Gerbino, S.; Siena, L.; Gjomarkaj, M.; Pace, E. Dual Anti-Oxidant and Anti-Inflammatory Actions of the Electrophilic Cyclooxygenase-2-Derived 17-Oxo-DHA in Lipopolysaccharide- and Cigarette Smoke-Induced Inflammation. *Biochim. Biophys. Acta BBA - Gen. Subj.* **2014**, *1840* (7), 2299–2309.

(63) Haeggström, J. Z.; Funk, C. D. Lipoxygenase and Leukotriene Pathways: Biochemistry, Biology, and Roles in Disease. *Chem. Rev.* **2011**, *111* (10), 5866–5898.

(64) Jónasdóttir, H. S.; Ioan-Facsinay, A.; Kwekkeboom, J.; Brouwers, H.; Zuurmond, A.-M.; Toes, R.; Deelder, A. M.; Giera, M. An Advanced LC–MS/MS Platform for the Analysis of Specialized Pro-Resolving Lipid Mediators. *Chromatographia* **2015**, *78* (5), 391–401.

(65) van Rooden, E. J.; Florea, B. I.; Deng, H.; Baggelaar, M. P.; van Esbroeck, A. C. M.; Zhou, J.; Overkleeft, H. S.; van der Stelt, M. Mapping *in Vivo* Target Interaction Profiles of Covalent Inhibitors Using Chemical Proteomics with Label-Free Quantification. *Nat. Protoc.* **2018**, *13* (4), 752–767.
(66) Soethoudt, M.; Stolze, S. C.; Westphal, M. V.; van Stralen, L.; Martella, A.; van Rooden, E. J.; Guba, W.; Varga, Z. V.; Deng, H.; van Kasteren, S. I.; Grether, U.; IJzerman, A. P.; Pacher, P.; Carreira, E. M.; Overkleeft, H. S.; Ioan-Facsinay, A.; Heitman, L. H.; van der Stelt, M. Selective Photoaffinity Probe That Enables Assessment of Cannabinoid CB2 Receptor Expression and Ligand Engagement in Human Cells. *J. Am. Chem. Soc.* **2018**, *140* (19), 6067–6075.
(67) Rappsilber, J.; Mann, M.; Ishihama, Y. Protocol for Micro-Purification, Enrichment, Pre-Fractionation and Storage of Peptides for Proteomics Using StageTips. *Nat. Protoc.* **2007**, *2* (8), 1896–1906.
(68) Morcillo, S. P.; Leboeuf, D.; Bour, C.; Gandon, V. Calcium-Catalyzed Synthesis of Polysubstituted 2-Alkenylfurans from β-Keto Esters Tethered to Propargyl Alcohols. *Chem. – Eur. J.* **2016**, *22* (47), 16974–16978.
(69) Walko, M.; Hewitt, E.; E. Radford, S.; J. Wilson, A. Design and Synthesis of Cysteine-Specific Labels for Photo-Crosslinking Studies. *RSC Adv.* **2019**, *9* (14), 7610–7614.
(70) Ravindar, K.; Sridhar Reddy, M.; Deslongchamps, P. A Highly Efficient Access to Spiroketals, Mono-Unsaturated Spiroketals, and Furans: Hg(II)-Catalyzed Cyclization of Alkyne Diols and Triols. *Org. Lett.* **2011**, *13* (12), 3178–3181.
(71) Tang, W.; Prusov, E. V. Total Synthesis of RNA-Polymerase Inhibitor Ripostatin B and 15-Deoxyripostatin A. *Angew. Chem. Int. Ed.* **2012**, *51* (14), 3401–3404.
(72) Köpfer, A.; Breit, B. Rhodium-Catalyzed Hydroformylation of 1,1-Disubstituted Allenes Employing the Self-Assembling 6-DPPon System. *Angew. Chem. Int. Ed.* **2015**, *54* (23), 6913–6917.
(73) Ramella, V.; He, Z.; Daniliuc, C. G.; Studer, A. Palladium-Catalyzed Dearomatizing Difunctionalization of Indoles and Benzofurans. *Eur. J. Org. Chem.* **2016**, *2016* (13), 2268–2273.